University of the Witwatersrand,
Johannesburg South Africa

A dissertation submitted in the fulfilment of the requirement for the Master of Science in the school of physics

Quasinormal modes for a spin-3/2 field in a Reissner-Nordstrøm background

Author:
Mr. Xolane Ignitious Ngcobo

Supervisor:
Prof. Alan Cornell
Co-Supervisor
Prof. Robert de Mello Koch

Abstract

In this dissertation I will present quasinormal mode results calculated using two approximation methods; the *Wentzel-Kramers-Brillouin* (WKB) and the *Asymptotic iteration method* (AIM). I will first do two brief examples, where we will compute the QNMs for a scalar field in a Schwarzschild and Reissner-Nordstrϕm background, then the QNMs for a massless Dirac spinor in a Schwarzschild background. These two examples will help build some intuition leading up to the main subject of this dissertation - the spin-3/2 field. The use of the WKB method is motivated by the works of *Sai Iyer* and *Clifford M. Will* [1], where they applied the WKB approximation method to computing the QNMs for black holes perturbed by fields. The AIM approximation method used here is the improved AIM approach of Cho et al [2]. This work is aimed at understanding the behaviour of spin-3/2 field in a blackhole background, and since the Schwarzschild background for the spin-3/2 has been intensively studied, I have decided that the Reissner-Nordstrϕm background will be very interesting to study as it is a charged background.

Declaration

This dissertation is a presentation of my original research work. Wherever contributions of others are involved, every effort is made to indicate this clearly, with due reference to the literature, and acknowledgement of collaborative research and discussions. The work was done under the guidance of Prof. Alan Cornell and Prof. Robert De Mello Koch, at the University of the Witwatersrand, Johannesburg South Africa.

AUTHOR'S SIGNATURE : ....

DATE : ....

Preface

The contents of this dissertation were presentated, by the author(s), at the following platforms:

Article:

- Chen C-H, Cho H-T, Cornell A.S, Harmsen G-H, and Ngcobo X.I, "Quasinormal modes for a spin-3/2 field in a Reissner-Nordstrom black hole background", arXiv:1710.08024, (2017).

Proceedings:

- South African Institute of Physics (SAIP) where a discussion of QNMs for scalar fields, Dirac fields and as well as a discussion on how to compute QNMs for a spin-3/2 field. The proceedings for this workshop will be published in the 2017 SAIP journal and the title for the work presented in the workshop is "Quasinormal modes for a spin-3/2 field in the Reissner-Nordstrøm black hole background".
- High Energy Particle Physics (HEPP) Wits workshop where a discussion of the QNMs for a spin-3/2 field was presented. The proceedings to this discussion will be published on the 2017 HEPP journal, and the title to this work is "Quasi normal modes for a spin-3/2 field in a 4-dimensional Reissner-Nordstr öm black hole background".

Acknowledgments

I would like to thank the overwhelming support of Prof. Alan Cornell, my supervisor, for all the inspiration and lessons (time management being the important one) I have learned working with him. I would also like to thank Prof. Robert de Mello Koch for all his *advanced quantum field theory* lectures and for providing me with his research grant in order to fund this work. I also thank Gerhard Harmsen for all the assistance he gave me and all the fruitful conversations we had. The support from my family, my mother in particular, and colleagues will not go unnoticed. I thank each and everyone of them.

Last but not least I would like to thank the University of the Witwatersrand, School of Physics, for granting me the opportunity to be part of a very big, friendly, and extremely dedicated family. Being in the presence of the staff and students alike served as great motivation.

To my mother

Sbongile Victoria Ngcobo

and my late father

Simphiwe Knowledge Ngcobo

(1949 - 2006)

Contents

List of Tables

Definitions and conventions

To make sure that we communicate our work clearly and that there is no ambiguity in the interpretation we will define few converntions and notation. In this dissertation we will be using natural units for all calculations, that is Table 1:

$G = 1$	Newton's Constant
$k_e = 1$	Coulomb's constant
$\hbar = 1$	Planck's Constant
$c = 1$	The speed of light
$k_B = 1$	Boltzmann's constant
Abbriviations	**Full name**
TT	Transverse and Traceless

Table 1: *Natural Constants*

Some of the important variables used throughout this dissertation are:

Variable	Meaning
r_s	Schwarzschild Radius
$r_\pm$	Reissner-Nordstr$\not{o}$m radii
Q	Charge of the black hole
M	Mass of the black hole
m	Mass of the field
ω	Quasinormal frequency
n	Harmonic number
l	Magnetic Quantum Number
J	Angular momentum
$g_{\mu\nu}$	Curved spacetime metric
g	Determinant of the curved spacetime metric
γ^μ	Gamma matrices

Table 2: *Variables and meaning*

We will be using the metric signature, $\eta_{\mu\nu} =$ and $(-1, 1, 1, 1)$, for all calculations peformed in this work.

Chapter 1

Introduction

1.1 Quasinormal modes

In this work we will be studying perturbations of black holes. Black holes themselves are simple objects that can be characterised by the angular momentum, the mass, and the charge of the black hole. We will look at these simple spacetime backgrounds perturbed by a variety of fields. These perturbations cause the surface of the event horizon of the black hole to oscillate. These oscillations give off damped modes, where we will be calculating the frequencies of these modes. The perturbations of black holes can result from matter interacting with the black hole or from the collapse (the death) of a star. Adding a perturbation to a black hole results in a disturbance of the system (the stable black hole) which, after some finite time, will establish some equilibrium by producing quasinormal modes (QNMs). Thus, when we are studying QNMs we get some information about the stability of the black hole. They are called "QNM" because there is a loss in energy as these modes propagate infinitely far away from the black hole. Unlike normal modes, where they are solutions to steady state systems, the QNMs are damped and we show this damping by assuming the ansatz,

$$\Psi \sim e^{-i\omega x}\,, \tag{1.1}$$

where ω - complex - are the quasinormal frequencies (QNFs), the frequencies associated with the modes. QNMs are everywhere, when you hit a glass and the particles around the glass vibrate (producing sound) and then return back to equilibrium configuration, you are producing QNMs. In fact, this is exactly what happens with a black hole. When the particle enters the black hole it causes the spacetime around the black hole to vibrate, these vibrations are the QNMs we are interested in studying. The main subject of this dissertation is the study of the Reissner-Nordstr$\o$m black hole perturbations due to spin-3/2 field.

The spin-3/2 particle theory approach we will be using in this dissertation is based on the work by W. Rarita and J. Schwinger [3], and based on the work by Fierz and Pauli in Ref. [4] on particle theory for arbitrary spin. There are other approaches to studying spin-3/2 particles, but these will not be mentioned in this work. The theory proposed by Rarita and Schwinger has it's shortcomings, one of these is the fact that the wave solutions to the Rarita-Schwinger equation propagates faster than the speed of light when it interacts with an electromagnetic field [5]. No one has ever detected a spin-3/2 particle before, but there are some strong arguments suggesting that spin-3/2 particle theory we are using describes the gravitino (the super particle partner of the graviton) field in theories of supergravity. This is one of the reasons we are interested in studying the QNMs due to these particles. Together with the field theory we need to develop the frame work for the black hole in which the field will interact. The tool that will help build the mathematical structure of the black hole is the theory of general relativity.

1.2 Spacetime backgrounds

Before we get into the main subject of the dissertation, we need to understand a few things about black holes and quantum field theory. Thus, we will begin by first studying the Einstein field equations [6]

$$R_{\mu\nu} - \frac{1}{2}\, R\, g_{\mu\nu} = 8\,\pi\, G\, T_{\mu\nu}\,, \tag{1.2}$$

where the black holes we are interested in are the solutions to these equations. The first solution to these equations was produced by Schwarzschild [7], which turned out to be a spherically symmetric non-rotating, and un-charged black hole. Further solutions were presented later, where charge and rotation were considered. In this dissertation we will only focus on two solutions; the Schwarzschild and the Reissner-Nordstrϕm solutions. The Reissner-Nordstrϕm solution is for a spherically symmetric, non-rotating but charged body discovered independently by both Reissner and Nordstrϕm [8, 9].

We will begin by considering a scalar field in a Schwarzschild black hole background then do a brief discussion of the scalar field in a Reissner-Nordstrϕm background. A scalar field is described by the *Klein-Gordon* equation of motion [10],

$$\left(\partial^{\mu}\partial_{\mu} + m^2\right)\Psi = 0. \tag{1.3}$$

This equation is true in flat spacetime, but we will have to "elevate" the equation to general curved spacetime backgrounds. Similarly, the Dirac spinor equation [11],

$$\left(i\gamma^{\mu}\partial_{\mu} - m\right)\Psi = 0, \tag{1.4}$$

is for flat spacetime and to get the correct modes in a curved background we will have to "elevate" this equation to a general curved spacetime. Lastly, the massless spin-3/2 field is described by the *Rarita-Schwinger equation*,

$$\gamma^{\mu\nu\rho}\nabla_{\nu}\Psi_{\rho} = 0, \tag{1.5}$$

which we will be using in a Reissner-Nordstrϕm background to compute the QNMs. In general it is very dificult to solve the equations of motion in order to compute the QNFs. We will use semi-analytical methods to approximate the solutions to the equations of motion and thus the QNFs.

1.3 Schrödinger-like equation

We are interested in the radial parts of the equations of motion describing the three sets of equations of motion (scalar, Dirac and spin-3/2). In order for us to make use of the *Wentzel-Kramers-Brilloin* (WKB) and the asymptotic iteration method (AIM) to approximate the QNMs, we must transform the radial equation to a Schrödinger-like equation,

$$\frac{d^2\Psi}{dx^2} + \big(\omega^2 - V(x)\big)\,\Psi = 0\,, \tag{1.6}$$

with the boundary conditions

$$\begin{aligned} V(x) &\to 0, \qquad \text{for} \qquad x \to -\infty \\ V(x) &\to 0, \qquad \text{for} \qquad x \to \infty\,. \end{aligned} \tag{1.7}$$

When computing the QNMs we follow this process:

- Write the quantum field theory in the specific spacetime we wish to study.
- Solve the equations of motion for the field.
- Use tortoise coordinates to transform the radial part to a Schrödinger-like "master" equation.
- Use the potential to then compute the QNMs.

It is very important that the master equation, the radial equation, is a Schrödinger-like equation. Recall that the WKB and AIM are both approximation methods for second order differential equations that look like Eq.(1.6) [12, 13].

We will also produce plots for the potential for all the cases and do a comparison. The QNMs can be used to compute various other properties of the black holes [14, 15], which we will not do in this work.

1.4 Outline

The outline of this work will be as follows:

We will first establish a foundation by introducing some mathematical concepts in chapter 2 which will be important for the overall work. In chapter 3 we will show a simple derivation and discussion of the Reissner-Nordstr$\o$m spacetime. With the mathematical tools and the Schwarzschild solutions to the Einstein equations we will, in chapter 4, derive the potential needed to calculate the QNMs for a scalar field in a D-dimensional Schwarzschild and Reissner-Nordstr$\o$m black hole background. In chapter 5 we shall review the cases of a Dirac field, before moving onto, the spin-3/2 field in a D-dimensional Reissner-Nordstr$\o$m black hole background in chapter 6. We shall derive the potential which we will then make use of to calculate the QNMs.

Note that the theoretical work which is set up, and the potentials we have found, will then be put into *Mathematica* to numerically compute the QNFs. We will list the QNFs calculated for the scalar field, massless Dirac spinor, and the spin-3/2 field, and then compare the results with some of the results in the literature. Finally, in chapter 7, we will give our concluding remarks on the subject of this dissertation and give some possible future work that can be done.

Chapter 2

Approximation tools for solving QNMs

2.1 WKB approximation method

The Wenzel, Krammers, Brilloum, and Jeffreys (JWKB) approximation method, sometimes referred to as the WKB, is used to find approximate solutions to linear differential equations with slowly varying coefficients [16]; in our case a Schrödinger-like equation with potential we shall determine case by case. The use of the WKB method is motivated by the fact that we can reduce the equations of motion for a particular field in some spacetime background to a "Schrödinger-like" second order differential equation. In some simple spacetime backgrounds, e.g the Schwarzschild background, the potential depends only on the parameters of the blackhole and not on the QNFs.

We will be interested in solving an equation of the type

$$\frac{d^2\Psi}{dx^2} + Q^2(x)\Psi = 0\,, \tag{2.1}$$

with $Q(x) = \sqrt{\omega^2 - V(x)}$ and $V(x)$ is a slowly varying function of "x". In order to use the WKB method, the potential must behave like a barrier and go to constant value as $x \to \pm\infty$. In Figure 2.1 we illustrate the type of potential function we need in order to be able to use the WKB method,

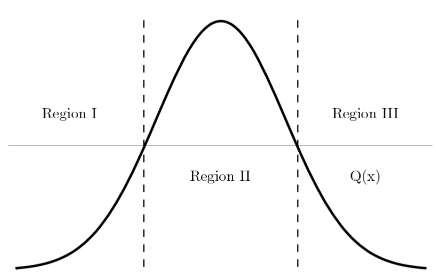

Figure 2.1: *Example of the type of barrier potential function needed for the WKB method to work.*

where the idea is to solve Eq.(2.1) in the regions I and III independently then write a Taylor series expansion in region II, and patch the solutions of these regions at the classical turning points, where the vertical dotted lines ing Figure 2.1.

The first time this method was used was when *Bernard Schutz* and *Clifford Will* computed the QNMs to third order for a scalar field in a Schwarzschild background Ref. [17], and was then improved by Konoplya Ref. [18] to sixth order, where we can now write the equation for the QNFs as:

$$\frac{i\left(\omega_n^2 - V_0\right)}{\sqrt{-2V_0''}} - \sum_{i=2}^{6} \Lambda_i = n + \frac{1}{2}\,, \tag{2.2}$$

where the Λ_i are constant coefficients that depend on the potential. While V_0 and V_0'' are the potential and the second derivative of the potential at some maximum point r_0, respectively.

2.2 Asymptotic iteration method - AIM

The AIM is an approximation method used to approximate solutions to second order differential equations of the type,

$$y'' = \lambda_0(x)y' + S_0(x)y\,, \tag{2.3}$$

with $\lambda_0(x) \neq 0$ and $s_0(x) \in C_\infty$. The motivation for us to use this approximation method in this work comes from the observation that obtaining QNMs involves solving a Schrödinger-like equation of the form,

$$\frac{d^2\Psi}{dx^2} + Q(x)\Psi = 0\,, \tag{2.4}$$

where the QNFs are embedded in the function $Q(x)$. Comparing Eq.(2.3) and Eq.(2.4) we realise that $\lambda_0(x) \to 0$ and $s_0(x) \to Q(x)$, we can then see that the problem we wish to tackle in this work qualifies to be analysed by the AIM [2]. Differentiating Eq.(2.3) with respect to the argument "x" gives

$$y'''(x) = \lambda_0'(x)y'(x) + \lambda_0(x)y''(x) + s_0'(x)y(x) + s_0(x)y'(x)\,. \tag{2.5}$$

Substituting Eq.(2.3) into the second term in the above equation and grouping all the $y'(x)$ and the $y(x)$ terms together we get that

$$y'''(x) = \lambda_1(x)y'(x) + s_1(x)y(x)\,, \tag{2.6}$$

with $\lambda_1(x) = \lambda_0(x) + s_0(x) + \lambda_0^2(x)$ and $s_1(x) = s_0(x) + s_0'(x)$. When we continue and differentiate Eq.(2.6) we get

$$y''''(x) = \lambda_2(x)y'(x) + s_2(x)y(x)\,, \tag{2.7}$$

where $\lambda_2(x) = \lambda_1'(x) + \lambda_1(x)\lambda_0(x) + s_1(x)$ and $s_2(x) = \lambda_1(x)s_0(x) + s_1'(x)$. We observe that we can write a general differential as

$$y^{(n+2)}(x) = \lambda_{(n)}(x)y'(x) + s_{(n)}(x)y(x)\,, \tag{2.8}$$

which requires that $\lambda_{(n)}(x) = \lambda'_{(n-1)}(x) + \lambda_0(x)\lambda_{(n-1)}(x) + s_{(n-1)}(x)$ and $s_{(n)}(x) = \lambda_{(n-1)}(x)s_0(x) + s'_{(n-1)}(x)$. At this point we introduce the the asymptotic bit of this method, which requires that

$$\frac{\lambda_{(n)}(x)}{s_{(n)}(x)} = \frac{\lambda_{(n-1)}(x)}{s_{(n-1)}(x)} \equiv \beta(x) \qquad \text{for}\, n\, \to \infty\,. \tag{2.9}$$

To solve Eq.(2.8) we take the ratio

$$\begin{aligned} \frac{y^{(n+2)}(x)}{y^{(n+1)}(x)} &= \frac{\lambda_{(n)}(x)y'(x) + s_{(n)}(x)y(x)}{\lambda_{(n-1)}(x)y'(x) + s_{(n-1)}(x)y(x)} \\ &= \frac{\lambda_{(n)}(x)}{\lambda_{(n-1)}(x)}\left[\frac{y'(x) + \frac{s_{(n)}(x)}{\lambda_{(n)}(x)}y(x)}{y'(x) + \frac{s_{(n-1)}(x)}{\lambda_{(n-1)}(x)}y(x)}\right]\,, \end{aligned} \tag{2.10}$$

and making use of the asymptotic information we get that

$$\frac{y^{(n+2)}(x)}{y^{(n+1)}(x)} = \frac{\lambda_{(n)}(x)}{\lambda_{(n-1)}(x)}\,. \tag{2.11}$$

With the observation that the ratio of $y^{(n+2)}(x)$ and $y^{(n+1)}(x)$ can be written as

$$\frac{y^{(n+2)}(x)}{y^{(n+1)}(x)} = \frac{d}{dx}\ln(y^{(n+1)}(x))\,, \tag{2.12}$$

we have then reduced the problem to solving the equation

$$\frac{d}{dx}\ln(y^{(n+1)}(x)) = \frac{\lambda_{(n)}(x)}{\lambda_{(n-1)}(x)}\,. \tag{2.13}$$

The solution, $y^{(n+1)}(x)$, can be found by simply integrating both sides of the equation. After integrating both sides we get

$$y^{(n+1)}(x) = k\, \exp\left\{\int\limits_x dx'\,\frac{\lambda_{(n)}(x')}{\lambda_{(n-1)}(x')}\right\}\,, \tag{2.14}$$

with k being a constant of integration. We can, furthermore, write

$$\frac{\lambda_{(n)}(x')}{\lambda_{(n-1)}(x')} = \frac{\lambda'_{n-1}(x) + \lambda_0(x)\,\lambda_{(n-1)}(x)}{\lambda_{(n-1)}} + \frac{s_{(n-1)}(x)}{\lambda_{(n-1)}(x)} = \lambda'_{(n-1)}(x) + \lambda_0(x) + \beta(x)\,, \tag{2.15}$$

with this result we can then write our solution as

$$y^{(n+1)}(x) = k\,\lambda_{(n-1)}(x)\exp\left\{\int\limits_x dx'\,[\lambda_0(x') + \beta(x')]\right\}\,. \tag{2.16}$$

The main objective of this exercise is to find the solution to Eq.(2.3), which means finding $y(x)$. We already know what $y^{(n+2)}(x)$ is, and thus we can simply substitute $y^{(n+2)}(x)$ into Eq.(2.8) and solve the differential equation. After substituting $y^{(n+2)}(x)$ into Eq.(2.8), the equation that we need to solve now is

$$k\,\lambda_{(n)}(x)\exp\left\{\int_x dx'\left[\lambda_0(x')+\beta(x')\right]\right\}=\lambda_{(n)}(x)y'(x)+s_{(n)}(x)y(x)\,. \tag{2.17}$$

Dividing the above equation by $\lambda_{(n)}$ and keeping in mind the definition of $\beta(x)$, we can then write

$$k\;\exp\left\{\int_x dx'\left[\lambda_0(x')+\beta(x')\right]\right\}=y'(x)+\beta(x)y(x)\,. \tag{2.18}$$

To solve this equation we write the solution as a sum of two parts, the homogeneous part and the particular solution part, as follows:

$$y(x)=y_h(x)+y_p(x)\,. \tag{2.19}$$

The homogeneous solution is given by solving the equation

$$y_h'(x)+\beta(x)y_h(x)=0\,. \tag{2.20}$$

To solve this equation we multiply both sides by the factor $\exp\left\{\int_x dx'\beta(x')\right\}$ and then group the left-hand side of the equation to get

$$\frac{d}{dx}\left[y_h(x)\int_x dx'\beta(x')\right]=0\,,$$

and the solution to this equation is given by

$$y_h(x)=C\exp\left\{-\int_x dx'\beta(x')\right\}\,. \tag{2.21}$$

Again C is just a constant of integration. To find $y_p(x)$ we assume the ansatz $y_p(x)=u(x)y_h(x)$, and since we know what $y_h(x)$ is, our task is to find the function $u(x)$ then we have our complete solution. Substituting the ansatz into Eq.(2.18)

$$k\;\exp\left\{\int_x dx'\left[\lambda_0(x')+\beta(x')\right]\right\}=u'(x)y_h(x)+u(x)y_h'(x)+\beta(x)u(x)y_h(x)\,. \tag{2.22}$$

Since we know that

$$y_h'(x)+\beta(x)y_h(x)=0\,,$$

we end up with a simplified equation

$$k\,\exp\left\{\int\limits_x dx'\left[\lambda_0(x')+\beta(x')\right]\right\} = u'(x)\left[C\exp\left\{-\int\limits_x dx'\beta(x')\right\}\right]\,, \tag{2.23}$$

to finally get

$$u'(x) = k\,\left[C_1\exp\left\{\int\limits_x dx''\beta(x'')\right\}\right]\exp\left\{\int\limits_x dx'\left[\lambda_0(x')+\beta(x')\right]\right\}\,, \tag{2.24}$$

and the solution to this equation is given by

$$u(x) = \int\limits_x dx' C_2\,\exp\left\{\int\limits_{x'} dx''\left[\lambda_0(x'')+2\beta(x'')\right]\right\}\,. \tag{2.25}$$

The final solution is just the summation of the homogeneous solution and the particular solution, which gives us the solution

$$y(x) = \exp\left\{-\int^x dx'\beta(x')\right\}\left[C + C_2\int^x dx'\exp\left\{\int^{x'} dx''\left[\lambda_0(x'')+2\beta(x'')\right]\right\}\right]\,. \tag{2.26}$$

To put this in perspective, we will look at one simple solvable example in the next subsection and solve it using the AIM, then compare the solutions.

2.2.1 Example

Consider the differential equation

$$y'' = 6y' - 5y\,, \tag{2.27}$$

where we see that in this example $\lambda_0(x) = 6$ and $s_0(x) = -5$. Since we are dealing with constant functions, $\lambda_n(x)$, $s_n(x)$ and their derivatives obviously vanish, which leads to the difference equations that determine $\lambda_n(x)$ and $s_n(x)$ to be

$$\lambda_n = \lambda_0\,\lambda_{(n-1)} + s_{(n-1)} \qquad \text{and} \qquad s_n = s_0\lambda_{(n-1)}\,. \tag{2.28}$$

We proceed by substituting $s_{(n-1)}$, λ_0, and s_0 into λ_n to get

$$\lambda_n = 6\,\lambda_{(n-1)} - 5\,\lambda_{(n-2)}\,. \tag{2.29}$$

Let $\lambda_n = a^n$ and substitute into Eq.(2.29):

$$\begin{aligned} a^n &= 6\,a^n\,a^{-1} - 5\,a^n\,a^{-2} \\ 0 &= a^2 - 6\,a + 5\,, \end{aligned} \tag{2.30}$$

which implies that $a = 5$ and $a = 1$, and thus

$$\lambda_n = A\,(5)^n + B\,, \tag{2.31}$$

where A and B are just constants. Now that we have the solution for λ_n, we can simply use it to compute s_n, since the relationship between the two is

$$s_n = -5\,\lambda_{(n-1)} = -5\,\left[A\,(5)^{(n-1)} + B\right]\,. \tag{2.32}$$

From Eq. (2.31) and Eq. (2.32), and the fact that $\lambda_0 = 6$ and $s_0 = -5$, we have

$$6 = A + B \qquad \text{and} \qquad -5 = -5\left[5^{-1}A + B\right]\,, \tag{2.33}$$

which leads to $A = 7$ and $B = -\frac{1}{4}$. Therefore

$$\lambda_n = \frac{1}{4}\left[28\,5^n - 1\right] \qquad \text{and} \qquad s_n = -\frac{5}{4}\left[\frac{28}{5}5^n - 1\right]\,, \tag{2.34}$$

and

$$\beta \equiv \lim_{n\to\infty} \frac{\lambda_n}{s_n} = -1\,.$$

It is now easy to proceed from this point since we have all the information we need to make use of Eq. (2.26). Substituting all the known parameters we get (for constants of integration C and C_2)

$$y(x) = C\,e^{x} + C_2\,e^{4x}\,. \tag{2.35}$$

2.2.2 Improved aymptotic iteration method

The draw back of the AIM is that every time one calculates the functions, $\lambda_n(x)$ and $s_n(x)$, one must first know the derivative of $\lambda_{n-1}(x)$ and $s_{n-1}(x)$. This will slow down the computation time if these functions are complicated. Luckily there is a way to solve this problem, where we write the Taylor expansion of these functions around the iteration point, ζ. The representation of the coefficients, $\lambda_n(x)$ and $s_n(x)$, can be expressed as:

$$\begin{aligned} \lambda_n(x) &= \sum_{i=0}^{\infty} c_n^i\,(x-\zeta)^i\,, \\ s_n(x) &= \sum_{i=0}^{\infty} d_n^i\,(x-\zeta)^i\,, \end{aligned} \tag{2.36}$$

where c_n^i and d_n^i are just the Taylor expansion coefficients. After substituting Eq.(2.36) into

$$\lambda_{(n)}(x) = \lambda'_{(n-1)}(x) + \lambda_0(x)\lambda_{(n-1)}(x) + s_{(n-1)}(x)\,,$$

and

$$s_{(n)}(x) = \lambda_{(n-1)}(x)s_0(x) + s'_{(n-1)}(x)\,,$$

we get the final recursion relation;

$$
\begin{aligned}
c_n^i &= (i+1)\, c_{n-1}^{i+1} + d_{n-1}^i + \sum_{k=0} c_0^k\, c_{n-1}^{i-k}\,, \\
d_n^i &= (i+1)\, d_{n-1}^{i+1} + \sum_{k=0}^{i} d_0^k c_{n-1}^{i-k}\,.
\end{aligned}
\tag{2.37}
$$

Using the AIM quantisation relation [19, 20] we find that we can compute the QNMs by studying the equation

$$
d_n^0 c_{n-1}^0 - d_{n-1}^0 c_n^0 = 0\,, \tag{2.38}
$$

with the index "n" being the number of iterations.

Chapter 3

Black holes

Black holes are solution to the Einstein field equations. There are four of such black holes; the Schwarzschild, Kerr, Reissner-Nordstr$\o$m, and the Kerr-Newmann black holes. In this chapter we will be interested in building the metric that describes the Schwarzschild and the Reissner-Nordstr$\o$m black holes.

3.1 Principles of General Relativity (Black holes)

The motivation to develop the theory of general relativity came after Einstein published a revolutionary paper in 1905; the special theory of relativity [21]. The theory of special relativity sets a limit to how fast objects could travel, this did not agree with the Newtonian theory of gravity. According to Newtonian mechanics, gravity is an instantaneous force. This means, for example, if the sun would vanish now we should feel the ripple effects of the gravitational waves instantly. This violates the postulate of special relativity that the speed of light "c" is the upper bound for how fast signals could travel[1]; including gravitational waves.

After Einstein developed the theory of general relativity it turned out that there were "beasts" that live within the beautiful equations; black holes. Black holes are extremely dense regions of space, where potentially a star died (due to its own strong gravitational force) and collapsed in a very small region of space. The simplest case, the "hydrogen atom" of black holes, is the Schwarzschild black hole with the line element,

$$ds^2 = \left(1 - \frac{2M}{r}\right) dt^2 - \left(1 - \frac{2M}{r}\right)^{-1} dr^2 - r^2 d\Omega^2 \,, \tag{3.1}$$

where $r = 2M$ is called the Schwarzschild radius, r_s. Spacetime is then separated into two regions, the region $R > r_s$ and the region where $R \leq r_s$. Once light, or matter, enters the sphere (with radius $R \leq r_s$) around the black hole it is trapped in this region forever. The surface of this sphere is called the event horizon of a black hole. There

[1] In fact, it was known, before special relativity, that electromagnetic waves travel at "c" in vacuum according to Maxwell's equations.

has been discussions among physicists (mainly Leonard Susskind and Stephen Hawking[2]) about whether information is lost completely once it enters the event horizon [22, 23]. The Schwarzschild black hole has one event horizon while the Reissner-Norström has two event horizons.

3.2 Einstein field equations

In the theory of general relativity the Einstein field equations,

$$R_{\mu\nu} - \frac{1}{2}\,R\,g_{\mu\nu} = 8\,\pi\,G\,T_{\mu\nu}\,, \tag{3.2}$$

describe how massive objects curve spacetime and how the curvature of spacetime dictates how objects then move in the spacetime. In Eq. (3.2), $R_{\mu\nu}$ is the Ricci tensor[3] calculated from the Reimann tensor

$$R^{\alpha}_{\mu\lambda\nu} = \partial_\lambda \Gamma^{\alpha}_{\mu\nu} - \partial_\nu \Gamma^{\alpha}_{\mu\lambda} + \Gamma^{\alpha}_{\lambda\rho}\Gamma^{\rho}_{\mu\nu} - \Gamma^{\alpha}_{\nu\rho}\Gamma^{\rho}_{\lambda\mu}\,. \tag{3.3}$$

By taking the trace of the Ricci tensor, we get the Ricci scalar $R = g^{\mu\nu}R_{\mu\nu}$. The "matter" part of the equation is given by the energy-momentum tensor $T_{\mu\nu}$. This implies that if one knows the matter populating the universe, $T_{\mu\nu}$, then one can, in principle, tell how curved the space is. Similarly, knowing how curved the space is, $R_{\mu\nu}$, we can say something about the matter populating the spacetime. The Γ's, also known as the connection coefficients, are computed from the metric of the spacetime as

$$\Gamma^{\alpha}_{\mu\nu} = \frac{1}{2}\,g^{\alpha\rho}\left\{\partial_\mu g_{\nu\rho} + \partial_\nu g_{\rho\mu} - \partial_\rho g_{\mu\nu}\right\}\,. \tag{3.4}$$

We have computed the above Christoffel symbols in appendix A, where the non-zero Christoffel symbols in a spherically symmetric 4-dimensional space are,

$$\boxed{\begin{array}{llll}
\Gamma^{t}_{rt} = \Gamma^{t}_{tr} = \dfrac{f'}{2f} & & & \\[2ex]
\Gamma^{r}_{tt} = \dfrac{f\,f'}{2} & \Gamma^{r}_{rr} = -\dfrac{f'}{2f} & \Gamma^{r}_{\theta\theta} = -r\,f & \Gamma^{r}_{\phi\phi} = -r\,f\sin^2\theta \\[2ex]
\Gamma^{\theta}_{r\theta} = \Gamma^{\theta}_{\theta r} = \dfrac{1}{r} & \Gamma^{\theta}_{\phi\phi} = -\sin\theta\cos\theta. & &
\end{array}} \tag{3.5}$$

Some of the most well known solutions to the Einstein field equations are the Schwarzschild and the Reissner-Norström metrics given by the line elements,

$$ds^2 = \left(1 - \frac{2M}{r}\right)dt^2 - \left(1 - \frac{2M}{r}\right)^{-1} dr^2 - r^2 d\Omega^2 \tag{3.6}$$

and

[2]Susskind argued that the loss of information as explained by Hawking in the "information paradox" violates the foundation of quantum mechanics

[3]The Ricci tensor gives us the information about the curvature of spacetime.

$$ds^2 = \left(1 - \frac{2M}{r} + \frac{Q}{r^2}\right) dt^2 - \left(1 - \frac{2M}{r} + \frac{Q}{r^2}\right)^{-1} dr^2 - r^2 d\Omega^2\,, \tag{3.7}$$

respectively. In 4-dimensions, $d\Omega^2 = d\theta^2 + \sin^2\theta\, d\phi^2$ and Q is just the charge of the black hole.

3.3 Reissner-Nordstr$\not{o}$m black holes

The static solution to the Einstein field equations we will discuss at length, is the Reissner-Nordstr$\not{o}$m solution. This solution describes the spacetime around a charged body. The difference between this solution and the Schwarzschild solution is that now our body (the black hole) is charged, and everything else remains the same. Unlike the Schwarzschild case, the energy-momentum tensor does not vanish and thus we will be solving the field equations

$$R_{\mu\nu} - \frac{1}{2} R g_{\mu\nu} = T_{\mu\nu}\,, \tag{3.8}$$

where the charge will be given the terms of $T_{\mu\nu}$. This energy-momentum tensor is given in terms of the electromagnetic field strength tensor, $F_{\mu\nu}$, in the form [24],

$$T_{\mu\nu} = F_{\mu\rho} F^{\rho}_{\nu} - \frac{1}{4} g_{\mu\nu} F_{\rho\sigma} F^{\rho\sigma}\,, \tag{3.9}$$

where $F_{\mu\nu} = \partial_\mu A_\nu - \partial_\nu A_\mu$ and the energy-momentum has a zero trace. Therefore

$$\begin{aligned} T = g^{\mu\nu} T_{\mu\nu} &= g^{\mu\nu} F_{\mu\rho} F^{\rho}_{\nu} - \frac{1}{4} g^{\mu\nu} g_{\mu\nu} F_{\rho\sigma} F^{\rho\sigma} \\ &= F^{\nu}_{\rho} F^{\rho}_{\sigma} - F_{\rho\sigma} F^{\rho\sigma} \\ &= 0\,. \end{aligned} \tag{3.10}$$

We have used that for a 4-dimensional spacetime $g^{\mu\nu} g_{\mu\nu} = 4$, and the electromagnetic field strength tensor is symmetric with only the diagonal elements being non-zero. Following the procedure we used in deriving the Schwarzschild metric, we end up with the line element

$$ds^2 = -\left(1 - \frac{2M}{r} + \frac{Q}{r^2}\right) dt^2 + \left(1 - \frac{2M}{r} + \frac{Q}{r^2}\right)^{-1} dr^2 + r^2 d\Omega^2\,, \tag{3.11}$$

with singularities at

$$r_\pm = M \pm \sqrt{M^2 - Q^2}\,, \tag{3.12}$$

where $Q^2 \not> M^2$ and $Q^2 = M^2$ is the extremal case. We will be setting $M = 1$ in many cases later on and thus the extremal case will be when $Q = 1$ in these cases.

With the above formulated spacetime backgrounds we need to also formulate the mechanism of studying fields in these backgrounds. To do this, in the following section, we will introduce a mathematical tool that will allow us to write a transformation of field equations in flat spacetimes to curved spacetimes.

3.4 Higher dimensional Reissner-Nordstrϕm black hole

There has been a growing interest in studying higher dimensional black holes in physics. This is motivated by the fact that unification theories such as *String Theory* are $d > 4$ spcetime theories with gravity being part of these theories. As such, it becomes important to study the objects of Einstein gravity in $d > 4$ spacetime dimensions. Reference [25] suggests that higher dimensional black holes could be produced at places like the LHC, where it would be in our interests to study how QNMs for $d = 4$ spacetimes differ from QNMs produced by higher dimensional black holes.

Since we will be focusing on D-dimensional black holes, we have to write the metric of the Reissner-Nordstrϕm black hole in D-dimensions. From Ref.[26] we learn that,

$$f(r) = 1 - \frac{2M}{r} + \frac{Q}{r^2} \qquad \rightarrow \qquad f(r) = 1 - \frac{2M}{r^{(D-3)}} + \frac{Q}{r^{(2D-6)}} \qquad \text{and} \tag{3.13}$$

$$d\Omega^2 \qquad \rightarrow \qquad d\Omega^2_{D-2}\,, \tag{3.14}$$

where the line element for a D-dimensional Reissner-Norström black hole is

$$ds^2 = -f(r)dt^2 + f(r)^{-1}dr^2 + r^2 d\Omega^2_{D-2}\,. \tag{3.15}$$

$d\Omega^2_{D-2}$ is the line element for a $(D-2)$ sphere. The event horizon(s) of this higher dimensional black hole are given by when $f(r) = 0$, which results in the radii

$$r_{\pm} = \left(M \pm \sqrt{M^2 - Q^2}\right)^{\frac{1}{D-3}}\,. \tag{3.16}$$

3.5 Vielbein

In this work we will be studying spacetime backgrounds that are not flat but, in general, curved. We should be able to convert all flat spacetime objects to their equivalent curved spacetime objects. To achieve this task we will develop a mathematical tool set called the *vielbein* that will help map flat spacetime to curved spacetime.

In developing this mathematical tool we begin by requiring that we denote the coordinate independent tetrads by $\hat{e}_a$, which then allows us to write the coordinate dependent tetrad as

$$\hat{e}_\mu(x) = e^a_\mu(x)\,\hat{e}_a\,. \tag{3.17}$$

The connecting matrix, $e^a_\mu(x)$, which is also known as the vielbein is an $N \times N$ matrix. These vielbein are chosen to satisfy the following mathematical relations [27],

$$e^a_\mu(x)\,e^\mu_b(x) = \delta^a_b \qquad \text{and} \qquad e^a_\mu(x)\,e^\nu_a(x) = \delta^\nu_\mu\,, \tag{3.18}$$

and they relate the curved spacetime metric, $g_{\mu\nu}$, and the flat spacetime metric, η_{ab}, in the following way

$$g_{\mu\nu} = e^a_\mu \, e^b_\nu \, \eta_{ab} \, . \tag{3.19}$$

We can also write, from Eq. (3.19), the inverse vielbein relation as

$$g_{\mu\nu} \, e^\mu_a \, e^\nu_b = \eta_{ab} \, . \tag{3.20}$$

Taking the latin index a to denote flat spacetime and the greek index μ to denote curved spacetime, we notice that the vielbein act as a bridge from flat spacetime and the other leg in curved spacetime. Thus, we can take an object in flat spacetime and promote it into curved spacetime by the appropriate use of these vielbein. One of such example will be how we map the flat spacetime Dirac gamma matrices,

$$\gamma^0 = \begin{pmatrix} \mathbb{I} & \mathbf{0} \\ \mathbf{0} & \mathbb{I} \end{pmatrix} \qquad \text{and} \qquad \gamma^i = \begin{pmatrix} \mathbf{0} & \sigma^i \\ \sigma^i & \mathbf{0} \end{pmatrix} \tag{3.21}$$

where $\mathbb{I}$ is a 2×2 identity matrix and σ^i are the 2×2 Pauli matrices given by,

$$\sigma^1 = \begin{pmatrix} 0 & 1 \\ 1 & 0 \end{pmatrix} \quad , \quad \sigma^2 = \begin{pmatrix} 0 & -i \\ -i & 0 \end{pmatrix} \quad \text{and} \quad \sigma^3 = \begin{pmatrix} 1 & 0 \\ 0 & -1 \end{pmatrix} , \tag{3.22}$$

into the curved spacetime Dirac gamma matrices,

$$\gamma^\mu = e^\mu_a \, \gamma^a \, . \tag{3.23}$$

With this knowledge, it is then easy for us to write the normal massless Dirac equation

$$i\gamma^a \partial_a \Psi = 0 \, , \tag{3.24}$$

where γ^μ are the flat space gamma matrices, in curved spacetime as

$$i\gamma^\mu \nabla_\mu \Psi = 0 \, , \tag{3.25}$$

where $\gamma^\mu = e^\mu_a \gamma^a$ and the covariant derivative $\nabla_\mu = \partial_\mu + \Gamma_\mu$. Here the objects, Γ_μ, are the spin connection [4]. We need this formalism so that we can write the gamma matrices in curved spacetime, since the Rarita-Schwinger equation,

$$\gamma^{\mu\nu\rho} \nabla_\mu \Psi_\nu(x) = 0 \, , \tag{3.26}$$

makes use of the gamma matrices in curved spacetime. Also, we need to be able to write the covariant derivative in curved spacetime, see chapter 5 and 6 for more details.

[4] spin-connections allow us to write covariant derivatives in curved spacetime

Chapter 4

Scalar field

The focus of this chapter is the study of the real scalar field in two different D-dimensional spacetime backgrounds; the Schwarzschild and Reissner-Nordstrϕm backgrounds. We will begin by writing down the equations of motion for a scalar field in a general D-dimensional spacetime, then analyse these equations in the two spacetime backgrounds we are interested in. We will then apply the AIM and the WKB approximation methods to compute the QNFs, and do a comparison with literature.

A scalar field is a spin-0 field that can be described by the Klein-Gordon equation,

$$\left(\Box + m^2\right)\phi(x) = 0\,, \tag{4.1}$$

for a Minkowski spacetime background. Our first task will be to find the equivalent form of the Klein-Gordon equation for a Schwarzschild background. To do this, we proceed by looking at the Lagrangian density for the scalar field in a more general spacetime background. The Lagrangian density is given as,

$$\mathcal{L} = \frac{\sqrt{-g}}{2}\,\left[\partial^{\mu}\phi\,\partial_{\mu}\phi - m^2\phi^2\right]\,, \tag{4.2}$$

with "g" being the determinant of the metric. The determinant for the Minkowski spacetime metric, $\eta_{\mu\nu}\,=\,\mathrm{diag}\,(-1,\,1,\,1,\,1)$, is $g\,=\,-1$ and thus Eq.(4.2) reduces to the Lagrangian density for flat 4-dimensional spacetime,

$$\mathcal{L} = \frac{1}{2}\,\left[\partial^{\mu}\phi\,\partial_{\mu}\phi - m^2\phi^2\right]\,. \tag{4.3}$$

4.1 Equations of motion

In classical field theory we use the Euler-Lagrangian equation,

$$\partial_{\mu}\left(\frac{\partial\,\mathcal{L}}{\partial\left(\partial_{\mu}\phi\right)}\right) = \frac{\partial\,\mathcal{L}}{\partial\phi}\,, \tag{4.4}$$

when we wish to compute the equations of motion for a given Lagrangian density. For the real scalar field in a general spacetime, the right side of Eq. (4.4) is

$$\frac{\partial\,\mathcal{L}}{\partial\phi} = -\sqrt{-g}\,m^2\phi\,,$$

and the left side of Eq. (4.4) is

$$\partial_\mu \left(\frac{\partial \mathcal{L}}{\partial \left(\partial_\mu \phi\right)} \right) = \partial_\mu \left[\sqrt{-g}\, g^{\mu\nu} \partial_\nu \phi \right] \, .$$

Combining these results we get that the equations of motion for a general spacetime with metric $g_{\mu\nu}$ and determinant g as

$$\left[\frac{1}{\sqrt{-g}} \partial_\mu \left[\sqrt{-g}\, g^{\mu\nu} \partial_\nu \right] + m^2 \right] \phi = 0 \, . \tag{4.5}$$

We now have the equation of motion for a real massive scalar field in a general spacetime. Our focus, however, is to study how the real massless ($m \to 0$) scalar field behaves in Schwarzschild or Reissner-Nordstr$\not{o}$m spacetime backgrounds, and eventually solve Eq. (4.5) .

4.2 Schwarzschild Background

In this section we will employ results from Chapter 3 and the previous section to build some intuition on how the spacetime around the neighborhood of the Schwarzschild black hole would respond if a scalar particle was to "fall into" the black hole. To achieve this task, we will solve Eq. (4.5) and do the analysis of the results.

We have seen that the metric for a D-dimensional Schwarzschild spacetime is given by the line element

$$ds^2 = -f(r)dt^2 + f(r)^{-1} dr^2 + r^2 d\Omega^2_{D-2}$$

with $f(r) = 1 - 2M/r^{(D-3)}$, M is the mass of the black hole. What we are aiming at solving is the equation,

$$\frac{1}{r^{D+2}} \frac{d}{dr} \left(r^{D+2} \frac{dR}{dr} \right) + \left[\omega^2 - \frac{l(l+D+1)}{r^2} \right] R = 0 \tag{4.6}$$

but we observe that for all $\mu \neq \nu$, $g^{\mu\nu} = 0$, and thus the above equation simplifies greatly. We will employ the method of separation of variables to solve Eq.(4.6). We write the ansatz,

$$\Psi = e^{-i\omega\, t} R(r) Y(\theta, \phi) \, , \tag{4.7}$$

which is motivated by Eq.(4.6). The radial part can be writen as a one-dimensional Schrödinger-like equation by introducing tortoise coordinates, see Appendix 2, as

$$\hat{R} = \frac{R}{r} \qquad \text{and} \qquad dx = \frac{r}{r - 2M} dr \, . \tag{4.8}$$

with this substitution the radial equation then assumes the final equation, which looks like a Schrödiner equation,

$$\frac{d^2 \hat{R}}{dx^2} + \left(\omega^2 - V \right) \hat{R} = 0, \tag{4.9}$$

where

$$V = f(r)\left[\frac{l(l+1)}{r^{D-2}} - \frac{2M}{r^{2D-3}}\right]. \tag{4.10}$$

The tortoise coordinates also allow one to map the event horizon to $-\infty$. We observe that, given the tortoise coordinates, the line element is now given by

$$ds^2 = \left(1 - \frac{2M}{r(x)}\right)\left(-dt^2 + dx^2\right) + r^2(x)d\Omega^2 . \tag{4.11}$$

To compute the QNMs for the scalar field we will be interested in the above potential Eq.(4.10). The angular part of the master equation can be further separated by requiring $Y(\theta,\phi) = e^{im\phi}A_{lm}(\theta)$. Where we realise that $A_{lm}(\theta)$ satisfies the spherical harmonic equation, and $A_{lm}(\theta)\ \forall\ \theta\ \epsilon\ [0,\pi]$ gives the constant $\lambda = l(l+1)$, where l and $|m| \leqslant l$ are integers.

4.3 WKB results

What we need to generate the QNFs is the master equation, which is given by Eq.(4.9), and the potential given by,

$$V = f(r)\left[\frac{l(l+1)}{r^{D-2}} - \frac{2M}{r^{2D-3}}\right] . \tag{4.12}$$

Graphically, the potential looks like (for $D \epsilon [4,8]$):

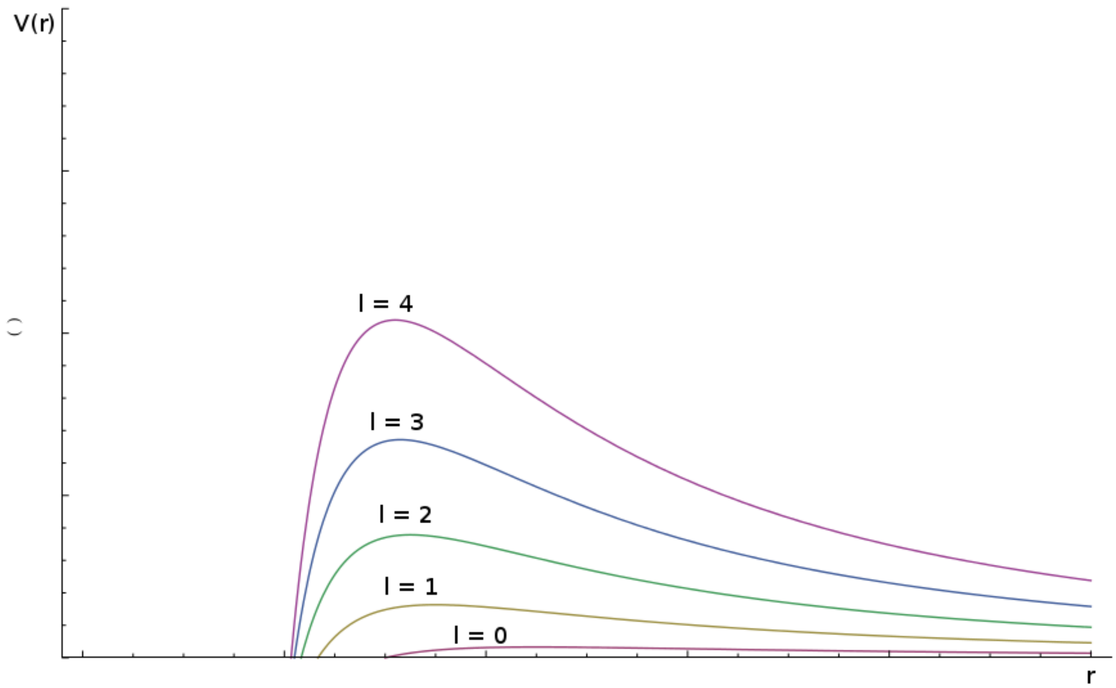

Figure 4.1: *A graph representing the scalar field potential $V(r))$ for $D = 4,5,6,7,8$*

We are now in a position to use the approximation methods we developed earlier to find the numerical values of the QNFs for the above potential. We will be interested in the 3rd order and the 6th order approximations to compute how damped the QNMs are.

l	n	WKB 3rd order	WKB 6th order
0	0	0.104647 - 0.1151970i	0.110463 - 0.1008200i
1	0	0.291114 - 0.0980014i	0.292910 - 0.0977616i
1	1	0.262212 - 0.3074320i	0.264471 - 0.3065180i
2	0	0.483211 - 0.0968049i	0.483642 - 0.0967661i
2	1	0.463192 - 0.2958100i	0.463847 - 0.2956270i
2	2	0.431660 - 0.5034330i	0.430386 - 0.5087000i
3	0	0.675206 - 0.0965121i	0.675366 - 0.0965006i
3	1	0.660414 - 0.2923440i	0.660671 - 0.2922880i
3	2	0.634839 - 0.4941180i	0.633591 - 0.4960110i
3	3	0.602182 - 0.7010530i	0.598429 - 0.7113850i
4	0	0.867340 - 0.0963964i	0.867416 - 0.0963919i
4	1	0.855684 - 0.2908990i	0.855808 - 0.2908770i
4	2	0.834492 - 0.4895220i	0.833684 - 0.4903220i
4	3	0.806392 - 0.6926510i	0.803186 - 0.6974820i
4	4	0.773068 - 0.8993250i	0.767217 - 0.9142280i
5	0	1.059570 - 0.0963389i	1.059610 - 0.0963368i
5	1	1.049970 - 0.2901650i	1.050040 - 0.2901540i
5	2	1.032010 - 0.4869570i	1.031500 - 0.4873430i
5	3	1.007480 - 0.6874410i	1.005170 - 0.6899180i
5	4	0.977892 - 0.8913410i	0.972776 - 0.8994900i
5	5	0.944128 - 1.0979100i	0.936349 - 1.1171400i

Table 4.1: *Scalar field QNF in a Schwarzschild black hole background for $D = 4$*

In table 4.1 we do a comparison between the QNFs computed using the WKB approximation method, in that we compare the results we obtained by using 3rd order and 6th order approximations. The 6th order approximation should lie closest to the true values for the QNFs. We notice also that the real values for the QNFs increases with the increase in angular quantum number "D" , higher modes are slightly more damped. In the following section we will introduce charge to the problem by considering a Reissner-Nordstrøm black hole background. We will perform similar calculations and investigate the effects of charge on the QNFs.

4.4 Reissner-Nordstrϕm Background

In this section we introduce a charged background to the problem above such that

$$f(r) = 1 - \frac{2M}{r^{D-3}} + \frac{Q^2}{r^{2(D-3)}} \,. \tag{4.13}$$

The calculations are similar to the ones we have studied in section 4.2, and as such, we will not go through a detailed derivation of the potential function. Starting from the general spacetime scalar field,

$$\frac{1}{\sqrt{-g}} \partial_\mu \left[\sqrt{-g}\, g^{\mu\nu} \partial_\nu \right] \phi = 0 \,, \tag{4.14}$$

and using the separation of variables method and tortoise coordinates, one arrives at the “Schrödinger-like” equation,

$$\frac{d^2}{dr^2} R + \left(w^2 - V(r) \right) R = 0 \,. \tag{4.15}$$

The potential now takes the form,

$$V(r) = f(r) \left[\frac{l\,(l+1)}{r^{2(D-3)}} + \frac{2M}{r^{3(D-3)}} - \frac{2Q^2}{r^{4(D-3)}} \right] , \tag{4.16}$$

which is similar to the Schwarzschild potential, with the addition of a charge term.

Again, using the potential function, we will carry out the numerical approximation calculations to obtain the QNFs for the Reissner-Nordstrϕm case of the scalar field. We will list, below, the QNFs for three case; $Q = 0.1\,, Q = 0.5\,,$ and $Q = 1\,.$ The physically acceptable values of Q are $Q \,\epsilon\, [0,\, 1] \times M$, where we have again set $M = 1$, and as such we will only look at QNFs of Q-values that lies in this region.

l	n	WKB 3rd order	WKB 6th order
0	0	0.104856 - 0.1152040i	0.110669 - 0.1008610i
1	0	0.291616 - 0.0980505i	0.293407 - 0.0978114i
1	1	0.262772 - 0.3075480i	0.265021 - 0.3066380i
2	0	0.484025 - 0.0968569i	0.484455 - 0.0968185i
2	1	0.464045 - 0.2959550i	0.464698 - 0.2957730i
2	2	0.432573 - 0.5036590i	0.431301 - 0.5089080i
3	0	0.676339 - 0.0965648i	0.676499 - 0.0965534i
3	1	0.661576 - 0.2924970i	0.661832 - 0.2924410i
3	2	0.636048 - 0.4943610i	0.634804 - 0.4962460i
3	3	0.603453 - 0.7013810i	0.599711 - 0.7116770i
4	0	0.868793 - 0.0964493i	0.868869 - 0.0964449i
4	1	0.857159 - 0.2910540i	0.857283 - 0.2910320i
4	2	0.836007 - 0.4897730i	0.835202 - 0.4905700i
4	3	0.807960 - 0.6929920i	0.804763 - 0.6978050i
4	4	0.774699 - 0.8997540i	0.768865 - 0.9146030i
5	0	1.061340 - 0.096392i	1.061390 - 0.096390i
5	1	1.051760 - 0.290322i	1.051830 - 0.290311i
5	2	1.033840 - 0.487212i	1.033320 - 0.487597i
5	3	1.009350 - 0.687790i	1.007050 - 0.690257i
5	4	0.979818 - 0.891780i	0.974718 - 0.899899i
5	5	0.946121 - 1.098440i	0.938363 - 1.117600i

Table 4.2: *Scalar field QNF in a Reissner-Nordstrøm ($Q = 0.1$, $M = 1$) black hole background in $D = 4$.*

The largest physical charge "Q", for this problem, we can study is $Q = 1$. We have chosen to compute QNFs for $Q = 0.1$, $Q = 0.5$, and $Q = 1$ so we can study the trend and get a feel of how the QNFs behave in the range $Q \,\epsilon\, [0, 1]$. There is a very strong agreement between the 3rd order and the 6th order WKB QNFs up to the second decimal place.

l	n	WKB 3rd order	WKB 6th order
0	0	0.110339 - 0.115049i	0.115800 - 0.1019520i
1	0	0.304891 - 0.0990835i	0.306551 - 0.0988743i
1	1	0.277636 - 0.3097880i	0.279707 - 0.3089830i
2	0	0.505561 - 0.0979773i	0.505966 - 0.0979492i
2	1	0.486684 - 0.2989870i	0.487306 - 0.2988410i
2	2	0.456898 - 0.5082680i	0.455756 - 0.5129970i
3	0	0.706317 - 0.0977058i	0.706469 - 0.0976977i
3	1	0.692368 - 0.2957520i	0.692615 - 0.2957070i
3	2	0.668200 - 0.4994520i	0.667091 - 0.5011410i
3	3	0.637378 - 0.7081750i	0.633953 - 0.7174320i
4	0	0.907253 - 0.097598i	0.907325 - 0.0975948i
4	1	0.896261 - 0.294399i	0.896381 - 0.2943820i
4	2	0.876242 - 0.495105i	0.875527 - 0.4958160i
4	3	0.849687 - 0.700148i	0.846784 - 0.7044550i
4	4	0.818261 - 0.908665i	0.812895 - 0.9220180i
5	0	1.108300 - 0.0975442i	1.10834 - 0.0975428i
5	1	1.099250 - 0.2937110i	1.09932 - 0.293703i
5	2	1.082290 - 0.4926810i	1.08183 - 0.493024i
5	3	1.059100 - 0.6951820i	1.05702 - 0.697383i
5	4	1.031150 - 0.9009970i	1.02650 - 0.908270i
5	5	0.999332 - 1.1094400i	0.992181 - 1.12667i

Table 4.3: *Scalar field quasinormal frequencies in a Reissner-Nordstrϕm ($Q = 0.5$, $M = 1$) black hole background in $D = 4$.*

We can immediately observe that the both 3rd order and 6th order WKB QNFs have increased with increase in charge. This indicates a direct proportionality relationship between the QNFs and charge in this problem. We are expecting that the following table will also indicate an increase in QNFs.

l	n	WKB 3rd order	WKB 6th order
0	0	0.121089 - 0.103712i	0.134402 - 0.0871679i
1	0	0.375703 - 0.089361i	0.377706 - 0.0893423i
1	1	0.343919 - 0.278285i	0.348314 - 0.275838i
2	0	0.626089 - 0.088728i	0.626574 - 0.0887508i
2	1	0.606772 - 0.269443i	0.608178 - 0.269098i
2	2	0.572535 - 0.457501i	0.572831 - 0.458166i
3	0	0.875936 - 0.088565i	0.876120 - 0.0885725i
3	1	0.862282 - 0.267257i	0.862851 - 0.267164i
3	2	0.836640 - 0.449993i	0.836787 - 0.450164i
3	3	0.801413 - 0.637760i	0.799021 - 0.640617i
4	0	1.12578 - 0.0884965i	1.12587 - 0.0884995i
4	1	1.11523 - 0.266406i	1.11551 - 0.266371i
4	2	1.09492 - 0.446830i	1.09500 - 0.446891i
4	3	1.06616 - 0.630759i	1.06482 - 0.631889i
4	4	1.03033 - 0.818460i	1.02575 - 0.823209i
5	0	1.37566 - 0.088461i	1.37571 - 0.0884627i
5	1	1.36706 - 0.265987i	1.36722 - 0.265972i
5	2	1.35030 - 0.445218i	1.35035 - 0.445245i
5	3	1.32614 - 0.626969i	1.32534 - 0.627496i
5	4	1.29551 - 0.811670i	1.29261 - 0.813961i
5	5	1.25926 - 0.999381i	1.25274 - 1.005870i

Table 4.4: *Scalar field quasinormal frequencies in a Reissner-Nordstrøm (Q = 1, M = 1) black hole background in $D = 4$.*

Note that we observe that the QNFs listed in tables 4.4 are larger than the ones for $Q = 0.5$ (table 4.4). This confirms the assumption we made above, we were expecting the QNFs to increase as we increase the charge. What this means is that, QNFs produced by a scalar field in a Reissner-Nordstrøm black hole background quickly vanish to infinitely as we increase the charge of the black hole. When the charge is small it will take some time for the same QNFs to vanish to infinitey.

Chapter 5

Spin-1/2 in a Schwarzschild background

The spin-1/2 particle is a Dirac particle described by the Dirac equation,

$$(i\gamma^{\mu}\partial_{\mu} + m)\,\Psi = 0\,. \tag{5.1}$$

The γ^{μ} are Dirac matrices and Ψ is a Dirac spinor. The line element for the chosen D-dimensional Schwarzschild background is given by

$$ds^2 = -\left(1 - \frac{2M}{r^{D-3}}\right) dt^2 + \left(1 - \frac{2M}{r^{D-3}}\right) dr^2 + r^2 d\Omega^2_{D-2}\,. \tag{5.2}$$

Since we are working in curved spacetime, the flat spacetime Dirac equation must be mapped to curved spacetime by using one of the mathematical tools we developed earlier, the *veilbeins*. The curved spacetime equation becomes

$$\left[i\gamma^{\mu}\left(\partial_{\mu} + \Gamma_{\mu}\right) + m\right]\Psi = 0\,, \tag{5.3}$$

where,

$$\Gamma_{\mu} = \frac{1}{8}\left[\gamma^{a}, \gamma^{b}\right] e^{\nu}_{\mu}\left(\partial_{\mu} e_{b\nu} - \Gamma^{\alpha}_{\mu\nu} e_{b\alpha}\right)\,,$$

which is the spin connection discussed in section 3.5.

In this work we will be interested in the massless ($m \to 0$) case of the Dirac equation, so the equation we are interested in solving is

$$\left[i\gamma^{\mu}\left(\partial_{\mu} + \Gamma_{\mu}\right)\right]\Psi = 0\,, \tag{5.4}$$

in the D-dimensional Schwarzschild background.

5.1 Equation of motion

When using the description in chapter 2, $\gamma^{\mu}\Gamma_{\mu}$ can be written as

$$\gamma^{a} e^{\mu}_{a}\Gamma_{\mu} = \gamma^{1}\, f^{1/2}\left(\frac{1}{r} + \frac{1}{4}\frac{f'}{f}\right) + \gamma^{2}\left(\frac{1}{2r}\right)\cot\theta\,, \tag{5.5}$$

where $f = \left(1 - 2M/r^{D-3}\right)$, which when we substitute into Eq. (5.4), we get the equation of motion

$$\begin{aligned} &\left\{\gamma^0\, f^{-1/2}\partial_t + \gamma^1 \left[f^{1/2}\left(\partial_r + \frac{1}{r} + \frac{1}{4}\frac{f'}{f}\right)\right]\right\}\Psi \\ &+ \left\{\gamma^2\left[\frac{1}{r}\left(\partial_\theta + \frac{1}{2}\cot\theta\right)\right] + \gamma^3\, r^{-1}\sin^{-1}\theta\,\partial_\phi\right\}\Psi = 0\,. \end{aligned} \tag{5.6}$$

We can further simplify the above equation by making the ansatz [28],

$$\Psi(t,r,\theta,\phi) \to f(r)^{-1/4}\phi(t,r,\theta,\phi)\,, \tag{5.7}$$

$$\begin{aligned} &\Rightarrow \gamma^0\, f^{-1/2}\partial_t f(r)^{-1/4}\phi + \gamma^1\left[f^{1/2}\left(\partial_r + \frac{1}{r} + \frac{1}{4}\frac{f'}{f}\right)\right] f(r)^{-1/4}\phi \\ &+ \gamma^2\left[\frac{1}{r}\left(\partial_\theta + \frac{1}{2}\cot\theta\right)\right] f(r)^{-1/4}\phi + \gamma^3\, r^{-1}\sin^{-1}\theta\,\partial_\phi f(r)^{-1/4}\phi = 0\,. \end{aligned} \tag{5.8}$$

After taking all the necessary derivatives and dividing throughout by $f(r)^{-1/4}$ we get the final simplified equation,

$$\frac{\gamma^0}{\sqrt{f}}\,\partial_t\phi + \gamma^1\left[\sqrt{f}\left(\partial_r + \frac{1}{r}\right)\right]\phi + \gamma^2\left[\frac{1}{r}\left(\partial_\theta + \frac{1}{2}\cot\theta\right)\right]\phi + \frac{\gamma^3}{r\,\sin\theta}\,\partial_\phi\phi = 0\,. \tag{5.9}$$

To continue we have to make an ansatz on how the Dirac bispinor, $\phi(t,r,\theta,\phi)$, should look like inorder to achieve the radial "Schrödinger-like" equation of motion. Making the ansatz [28, 29],

$$\phi(t,r,\theta,\phi) = \begin{pmatrix} \frac{i\,G^{(\pm)}(r)}{r}\,\chi^{(\pm)}_{jm}(\theta,\phi) \\ \frac{i\,F^{(\mp)}(r)}{r}\,\chi^{(\mp)}_{jm}(\theta,\phi) \end{pmatrix} e^{-i\omega t}\,, \tag{5.10}$$

where

$$\begin{aligned} \chi^{+}_{jm}(\theta,\phi) &= \begin{pmatrix} \sqrt{\frac{j+m}{2j}}Y_l^{m-1/2} \\ \sqrt{\frac{j-m}{2j}}Y_l^{m+1/2} \end{pmatrix} \qquad \text{for} \quad j = l + \frac{1}{2}\,, \\ \chi^{-}_{jm}(\theta,\phi) &= \begin{pmatrix} \sqrt{\frac{j+1-m}{2j+2}}Y_l^{m-1/2} \\ -\sqrt{\frac{j+1+m}{2j+2}}Y_l^{m+1/2} \end{pmatrix} \qquad \text{for} \quad j = l - \frac{1}{2}\,. \end{aligned} \tag{5.11}$$

As such, $Y_l^{m\pm1/2}(\theta,\phi)$ are just the solutions to the spherically symmetric part of the problem (simple spherical harmonics). With the coordinate shift,

$$r_* = r + 2M\ln\left(\frac{r^{D-3}}{2M} - 1\right)\,, \tag{5.12}$$

we can write the radial equation for $F^{\pm}$ and $G^{\pm}$ as

$$
\begin{aligned}
\frac{d}{dr_*}\begin{pmatrix} F^{\pm} \\ G^{\pm} \end{pmatrix} - \left(1-\frac{2M}{r^{D-3}}\right)^{1/2}\begin{pmatrix} \kappa_{\pm}/r & 0 \\ 0 & \kappa_{\pm}/r \end{pmatrix}\begin{pmatrix} F^{\pm} \\ G^{\pm} \end{pmatrix} \\
= \begin{pmatrix} 0 & -\omega \\ \omega & 0 \end{pmatrix}\begin{pmatrix} F^{\pm} \\ G^{\pm} \end{pmatrix}
\end{aligned}
\tag{5.13}
$$

with the integers, $\kappa_{\pm}$ given by

$$
\kappa_{\pm} = \begin{cases} -\left(j+1/2\right) & j = l+1/2 \\ \left(j-1/2\right) & j = l-1/2\,. \end{cases}
\tag{5.14}
$$

We will proceed by looking at the $(+)$ and $(-)$ cases separately. Let

$$
\begin{pmatrix} \hat{F}^{\pm} \\ \hat{G}^{\pm} \end{pmatrix} = \begin{pmatrix} \sin\left(\theta_+\right) & \cos\left(\theta_+/2\right) \\ \cos\left(\theta_+/2\right) & -\sin\left(\theta_+/2\right) \end{pmatrix}\begin{pmatrix} F^{\pm} \\ G^{\pm} \end{pmatrix},
\tag{5.15}
$$

which, when substituted into Eq.(5.13), leads to

$$
\frac{d}{dr_*}\begin{pmatrix} \hat{F}^{\pm} \\ \hat{G}^{\pm} \end{pmatrix} + W_{(+)}\begin{pmatrix} -\hat{F}^{\pm} \\ \hat{G}^{\pm} \end{pmatrix} = \omega\begin{pmatrix} \hat{G}^{\pm} \\ \hat{F}^{\pm} \end{pmatrix}
\tag{5.16}
$$

with

$$
W_+ = \left(1-\frac{2M}{r^{D-3}}\right)^{1/2}\left[\frac{\kappa_+}{r}\right].
\tag{5.17}
$$

The final decoupled radial equation of motion for the $(+)$ case is thus given by

$$
\begin{aligned}
\left(-\frac{d^2}{d\hat{r}_*^2} + V_{(+)1}\right)\hat{F}^{(+)} &= \omega^2\hat{F}^{(+)}\,, \\
\left(-\frac{d^2}{d\hat{r}_*^2} + V_{(+)2}\right)\hat{G}^{(+)} &= \omega^2\hat{G}^{(+)}\,,
\end{aligned}
\tag{5.18}
$$

with the potential function $V_{(+)1,2}$ given, in terms of W_+, as

$$
V_{(+)1,2} = \pm\frac{dW_{(+)}}{d\hat{r}_*} + W_{(+)}^2\,.
\tag{5.19}
$$

Similarly, the case for $(-)$ follows the same structure as the $(+)$ case. Following the same process we arrive at the equation,

$$
\begin{aligned}
\left(-\frac{d^2}{d\hat{r}_*^2} + V_{(-)1}\right)\hat{F}^{(-)} &= \omega^2\hat{F}^{(-)}\,, \\
\left(-\frac{d^2}{d\hat{r}_*^2} + V_{(-)2}\right)\hat{G}^{(-)} &= \omega^2\hat{G}^{(-)}\,.
\end{aligned}
\tag{5.20}
$$

Finally, we combine Eq.(5.18) and Eq.(5.20) to get

$$\left(-\frac{d^2}{d\hat{r}_*^2} + V_{1,2}\right)\hat{F} = \omega^2\hat{F}\,, \\ \left(-\frac{d^2}{d\hat{r}_*^2} + V_{1,2}\right)\hat{G} = \omega^2\hat{G}\,. \tag{5.21}$$

5.2 Results

Now that we have the potential, we will proceed as we did in the previous chapter. We will plot the potential function and also use the WKB method and AIM to compute the quasinormal frequencies.

4 Dimensions				
l	n	WKB 3rd order	WKB 6th order	AIM
0	0	0.176452-0.100109i	0.182646-0.0949346i	0.3233-0.1023i
1	0	0.378627-0.0965424i	0.380068-0.0963659i	0.5667-0.0955i
1	1	0.353604-0.298746i	0.355857-0.297271i	0.5497-0.2903i
2	0	0.573685-0.0963242i	0.574094-0.096307i	0.7809-0.0965i
2	1	0.556185-0.292981i	0.557016-0.292717i	0.7682-0.2916i
2	2	0.527289-0.497187i	0.526534-0.499713i	0.7445-0.4928i
3	0	0.767194-0.096276i	0.767354-0.0962705i	0.9897-0.0969i
3	1	0.753957-0.291048i	0.754300-0.290969i	0.9796-0.2921i
3	2	0.730450-0.490880i	0.729754-0.491909i	0.9603-0.4912i
3	3	0.699918-0.695711i	0.696729-0.702337i	0.9331-0.6964i
4	0	0.960215-0.0962564i	0.960293-0.0962539i	1.1960-0.0971i
4	1	0.949593-0.290179i	0.949759-0.290148i	1.1876-0.2923i
4	2	0.929979-0.487634i	0.92949-0.4881140i	1.1713-0.4903i
4	3	0.903578-0.689241i	0.901073-0.692513i	1.1479-0.6925i
4	4	0.872052-0.894412i	0.866729-0.905116i	1.1187-0.9005i
5	0	1.15303-0.0962463i	1.15307-0.096245i	1.4008-0.0972i
5	1	1.14416-0.2897140i	1.14425-0.28970i	1.3936-0.2924i
5	2	1.12741-0.485759i	1.12707-0.48601i	1.3795-0.4896i
5	3	1.10427-0.685156i	1.10246-0.686917i	1.3591-0.6901i
5	4	1.07614-0.887836i	1.07177-0.893883i	1.3331-0.8948i
5	5	1.04393-1.093240i	1.03664-1.107980i	1.3027-1.1048i

Table 5.1: *($n \leq l$, with $l = j - 1/2$) spin-1/2 field quasi normal mode frequencies using the WKB and the AIM methods with $D = 4$, $M = 1$.*

5 Dimensions				
l	n	WKB 3rd order	WKB 6th order	AIM
0	0	0.333820-0.182421i	0.182646-0.0949346i	0.3233-0.1023i
1	0	0.606143-0.176854i	0.380068-0.0963659i	0.5667-0.0955i
1	1	0.529285-0.561634i	0.355857-0.297271i	0.5497-0.2903i
2	0	0.863896-0.176815i	0.574094-0.096307i	0.7809-0.0965i
2	1	0.808054-0.544412i	0.557016-0.292717i	0.7682-0.2916i
2	2	0.718063-0.935957i	0.526534-0.499713i	0.7445-0.4928i
3	0	1.117150-0.176837i	0.767354-0.0962705i	0.9897-0.0969i
3	1	1.074370-0.538303i	0.754300-0.290969i	0.9796-0.2921i
3	2	0.999809-0.916313i	0.729754-0.491909i	0.9603-0.4912i
3	3	0.903378-1.30877i	0.696729-0.702337i	0.9331-0.6964i
4	0	1.368870-0.176828i	0.960293-0.0962539i	1.1960-0.0971i
4	1	1.334230-0.535484i	0.949759-0.290148i	1.1876-0.2923i
4	2	1.271220-0.906006i	0.92949-0.4881140i	1.1713-0.4903i
4	3	1.187250-1.28910i	0.901073-0.692513i	1.1479-0.6925i
4	4	1.086390-1.68196i	0.866729-0.905116i	1.1187-0.9005i
5	0	1.15303-0.0962463i	1.15307-0.096245i	1.4008-0.0972i
5	1	1.14416-0.2897140i	1.14425-0.28970i	1.3936-0.2924i
5	2	1.12741-0.485759i	1.12707-0.48601i	1.3795-0.4896i
5	3	1.10427-0.685156i	1.10246-0.686917i	1.3591-0.6901i
5	4	1.07614-0.887836i	1.07177-0.893883i	1.3331-0.8948i
5	5	1.04393-1.093240i	1.03664-1.107980i	1.3027-1.1048i

Table 5.2: *($n \leq l$, with $l = j - 1/2$) spin-1/2 field quasi normal mode frequencies using the WKB and the AIM methods with $D = 5$, $M = 1$.*

The QNFs we get using the 3rd, 6th order WKB approximation method and AIM increase as we increase the dimensions. Comparing tables 5.1 and 5.2 we see this change, increasing the dimensions increases both the real and the imaginary parts of the QNFs produced by the three approximation methods. The 6th order and AIM changes in both the real and the imaginary parts are small. Thus, the increase in dimensions for this problem has a noticeable difference on the 3rd order WKB compared to the 6th order and AIM.

Chapter 6

Spin-3/2 in a Reissner-Nordstr$\not{o}$m background

As with the previous two chapters, we begin our study of the spin-3/2 field by writing down the Lagrangian density as

$$\mathcal{L} = -\sqrt{-g}\,\bar{\psi}^{\mu}\,R_{\mu}\,, \tag{6.1}$$

with $R_{\mu} = \gamma_{\mu\nu\rho}\nabla^{\nu}\psi^{\rho} = \left(\nabla^{3/2} - \not{\nabla}\right)\psi_{\mu} - m\gamma_{\mu\nu}\psi^{\nu}$ [30]. The spin-3/2 derivative, $\nabla^{3/2}$, acting on ψ_{μ} gives the result:

$$\nabla^{3/2}\psi_{\mu} = \gamma_{\mu\nu\rho}\nabla^{\nu}\psi^{\rho} + \not{\nabla}\psi_{\mu}\,. \tag{6.2}$$

Plugging Eq.(6.2) into the Lagrangian density and keeping in mind the expression of R_{μ}, the Lagrangian density becomes,

$$\mathcal{L} = -\sqrt{-g}\bar{\psi}^{\mu}\left[\gamma_{\mu\nu\rho}\nabla^{\nu}\psi^{\rho} - m\gamma_{\mu\nu}\psi^{\nu}\right]\,, \tag{6.3}$$

such that taking $m \to 0$ and using the Euler-Lagrange equation of motion, we end up with the Rarita-Schwinger equation for a spin-3/2 field.

The field theory for spin-3/2 particles we will use was first formulated by W.Rarita and J.Schwinger in [3]. We will be using this description as the basis for our work. We are interested in the massless spin-3/2 particles, which are described by,

$$\gamma^{\mu\nu\rho}\,\nabla_{\nu}\Psi_{\rho} = 0\,, \tag{6.4}$$

where we require that the gamma matrices satisfy, see ref. [31],

$$\gamma^{\mu\nu\rho} = \gamma^{\mu}\gamma^{\nu}\gamma^{\rho} - \gamma^{\mu}g^{\nu\rho} + \gamma^{\nu}g^{\mu\rho} - \gamma^{\rho}g^{\mu\nu}\,. \tag{6.5}$$

Our choice of gamma matrices is given by,

$$\begin{aligned}
\gamma^{0} = i\sigma^{3}\otimes\mathbb{I} \quad &\Rightarrow \quad \gamma^{t} = \frac{1}{\sqrt{f}}\left(i\sigma^{3}\otimes\mathbb{I}\right)\\
\gamma^{i} = \sigma^{1}\otimes\bar{\gamma}^{i} \quad &\Rightarrow \quad \gamma^{\theta_i} = \frac{1}{r}\left(\sigma^{1}\otimes\bar{\gamma}^{\theta_i}\right)\\
\gamma^{3} = \sigma^{2}\otimes\mathbb{I} \quad &\Rightarrow \quad \gamma^{r}\sqrt{f}\left(\sigma^{2}\otimes\mathbb{I}\right)
\end{aligned} \tag{6.6}$$

with $i = 1, 2, ..., D-2$. The "bar" gamma matrices are those that live on a $(D-2)$-sphere. We are in fact interested in the "$\gamma^{\mu\nu\rho}$" gamma matrices, and we will use the definition in Eq.(6.5) to compute these gamma matrices. For $\mu \neq \nu \neq \rho$ the metric vanishes, and as we have,

$$\gamma^{\mu\nu\rho} = \gamma^{\mu}\gamma^{\nu}\gamma^{\rho} \,. \tag{6.7}$$

The non-vanishing γ matrices that we need for the Rarita-Schwinger equation are,

$$\begin{aligned}
\gamma^{t\theta_i r} &= -\frac{1}{r}\left(\mathbb{I}\otimes\bar{\gamma}^{\theta_i}\right) \\
\gamma^{t\theta_i\theta_j} &= \frac{1}{r^2\sqrt{f}}\left(i\sigma^3\otimes\bar{\gamma}^{\theta_i\theta_j}\right) \\
\gamma^{r\theta_j\theta_i} &= \frac{\sqrt{f}}{r^2}\left(\sigma^2\otimes\bar{\gamma}^{\theta_i\theta_j}\right) \,.
\end{aligned} \tag{6.8}$$

The wavefunction (in 4 dimensions), Ψ_ρ, is a 16 component spinor-vector which has 8 degrees of freedom needed to describe the spin 3/2 particle and it's anti-particle in 4-dimensions [32]. The objects that describe integral spin particles, like the photon, are tensors, and those that describe half integral spin particles, like the electron, are spinors. The object that describe spin-3/2 particles are a tensor product between the first rank tensor and the Dirac bispinor. Eq. (6.4) has the constraints,

$$\gamma^{\mu}\Psi_{\mu} = 0 \qquad \text{and} \qquad \partial^{\mu}\Psi_{\mu} = 0 \tag{6.9}$$

to eliminate the contribution of the spin-1/2 field in the Rarita-Schwinger equation. The covariant derivative ∇_ν acts on the vector-spinor Ψ_ρ in the following way:

$$\nabla_{\nu}\Psi_{\rho} = \partial_{\nu}\Psi_{\rho} + \frac{1}{4}\omega_{\nu}^{\sigma\lambda}\gamma_{\sigma\lambda}\Psi_{\rho} - \Gamma^{\beta}_{\rho\nu}\Psi_{\beta} \,, \tag{6.10}$$

where $\omega_{\nu}^{\sigma\lambda}$ is the spin connection given by the veilbein, see chapter 2, and $\Gamma^{\beta}_{\rho\nu}$ the Levi-Civita connections.

Before we proceed with the calculation of the equations of motion, we first have to make a few observations. The temporal and the radial components of the wavefunction are spinors on the 2-sphere, and as such we can write them as the inner product of some functions as follows:

$$\begin{aligned}
\Psi_t &= \psi_t \otimes \bar{\psi}_\lambda \qquad \text{and} \\
\Psi_r &= \psi_r \otimes \bar{\psi}_\lambda \,.
\end{aligned} \tag{6.11}$$

ψ_t is just a function that depends only on time and ψ_r is a function that only has radial dependence, while $\bar{\psi}_\lambda$ is an eigenfunction with eigenvalues $i\lambda$. The full study of the eigenfunctions, and thus the eigenvalues, was done by Camporesi and Higuchi [33]. The angular part of the Rarita-Schwinger equation takes a different form from the above $t-r$ equations. The reason is that the angular part does not behave like a spinor, but behaves like a spinor-vector on the $(D-2)$-sphere. As such, the angular equation takes takes the form

$$\Psi_{\theta_i} = \psi_\theta^{(1)} \otimes \bar{\nabla}_{\theta_i} \bar{\psi}_\lambda + \psi_\theta^{(2)} \otimes \bar{\gamma}_{\theta_i} \bar{\psi}_\lambda \,. \tag{6.12}$$

6.1 Eigenmodes and eigenvalues

In this section we will be interested in determining the eigenvalues of the spinor and spinor-vector, that describes the spin-3/2 field, on a D-dimensional sphere. We will begin by looking at the eigenvalues for the spinor and there after the spinor-vector.

6.1.1 Spinor eigenvalues

The study for determining the eigenvalues for the spinor in a S^D space can be broken down into two cases, that will eventually be linked together at the end. The first case will focus on the even D-dimensions, and the second case will be looking at the odd D-dimensions case.

D **even case:**

The covariant derivative, ∇_μ, acts on the spinor, ψ, in the following way:

$$\nabla_\mu \psi = \partial_\mu \psi + \omega_\mu \psi \,, \tag{6.13}$$

where ω_μ is the spin-connection (which is a consequence of our curved spacetime) and is given by

$$\omega_\mu = \frac{1}{2}\, \omega_{\mu ab} \Sigma^{ab} \tag{6.14}$$

$\Sigma^{ab} = \frac{1}{2}\left[\gamma^a, \gamma^b\right]$ and $\omega_{\mu ab}$ are given in terms of the veilbeins, as developed in Chapter 3, and their derivatives

$$\omega_{\mu ab} = e_a^\alpha \left(\partial_\mu e_{\alpha b} - \Gamma^\rho_{\mu\alpha} e_{\rho a}\right) \,. \tag{6.15}$$

D **odd case:**

In the case that we have odd numbered dimensions, our gamma matrices become

$$\gamma^D = \begin{pmatrix} \mathbf{1} & 0 \\ 0 & \mathbf{1} \end{pmatrix} , \tag{6.16}$$

while the non-vanishing spin-connection taking the form

$$\omega_{\theta_i} = \bar{\omega}_{\theta_i} - \frac{1}{2} \cos\theta_D \gamma^D \bar{\gamma}_{\theta_i} . \tag{6.17}$$

The eigenspinor equation becomes

$$\gamma^\mu \nabla_\mu \psi_\lambda = \left[\left(\partial_{\theta_D} + \frac{D-1}{2} \right) \gamma^D + \frac{1}{\sin\theta_D} \bar{\gamma}^{\theta_i} \bar{\nabla}_{\theta_i} \right] \psi_\lambda = i\lambda\psi_\lambda \,. \tag{6.18}$$

Now we have all the tools we need to calculate the equations of motion and the QNFs. The sections that follow will be dedicated at achieving these tasks.

6.2 Equations of motion

Now that the framework has been put in place, we are going to formulate the equation of motion for the massless spin-3/2 field. Using the Rarita-Schwinger equation we will have two solutions; the "Non-TT eigenmodes" and the "TT eigenmodes". These two solutions will provide us with two potential functions and thus two sets of QNFs.

6.2.1 TT eigenfunctions:

In this subsection we will rewrite the angular eigenfunction as

$$\Psi_{\theta_i} = \psi_\theta \otimes \bar{\psi}_{\theta_i} \,. \tag{6.19}$$

We will continue our calculations by recalling the Weyl gauge, $\psi_t = 0$, and the TT condition $\psi_r = 0$.
We will use these to simplify how we will calculate the equations of motion. These conditions, along with the angular eigenfunction, lead to the simplified equations of motion that is as follows:

$$\begin{aligned} &\left(\frac{1}{r\sqrt{f}}\, i\sigma^3 \partial_t + \frac{\sqrt{f}}{r}\sigma^2 \partial_r + \frac{f'}{4r\sqrt{f}}\sigma^2 + (D-4)\,\frac{\sqrt{f}}{2r^2}\sigma^2 \right)\psi_\theta + \\ &+ \left(i\frac{\bar{\xi}}{r^2}\sigma^1 - i\frac{Q}{2r^{D-1}}\sqrt{\frac{D-2}{2\,(D-3)}}\,\sigma^1 \right)\psi_\theta = 0\,, \end{aligned} \tag{6.20}$$

where Q is the charge of the black hole and $\bar{\xi} = j + (D-3)/2$ is the eigenvalue on the $(D-2)$-sphere. To proceed, we write

$$\psi_\theta = \sigma^2 \begin{pmatrix} \psi_{\theta_1} e^{-i\omega t} \\ \psi_{\theta_2} e^{-i\omega t} \end{pmatrix} , \tag{6.21}$$

$$\Rightarrow \quad \frac{1}{r\sqrt{f}}\, i\sigma^3\,\sigma^2 \begin{pmatrix} -i\omega\,\psi_{\theta_1} e^{-i\omega t} \\ -i\omega\,\psi_{\theta_2} e^{-i\omega t} \end{pmatrix} + \frac{\sqrt{f}}{r^2}\sigma^2\partial_r\,\sigma^2 \begin{pmatrix} -i\omega\,\psi_{\theta_1} e^{-i\omega t} \\ -i\omega\,\psi_{\theta_2} e^{-i\omega t} \end{pmatrix} +$$

$$\frac{f'}{4r\sqrt{f}} \begin{pmatrix} \psi_{\theta_1} e^{-i\omega t} \\ \psi_{\theta_2} e^{-i\omega t} \end{pmatrix} + (D-4)\,\frac{\sqrt{f}}{2r^2}\sigma^2\,\sigma^2 \begin{pmatrix} \psi_{\theta_1} e^{-i\omega t} \\ \psi_{\theta_2} e^{-i\omega t} \end{pmatrix} + \tag{6.22}$$

$$+\, i\frac{\bar{\xi}}{r^2}\sigma^1\,\sigma^2 \begin{pmatrix} \psi_{\theta_1} e^{-i\omega t} \\ \psi_{\theta_2} e^{-i\omega t} \end{pmatrix} - i\frac{Q}{2r^{D-1}}\sqrt{\frac{D-2}{2\,(D-3)}}\,\sigma^1\,\sigma^2 \begin{pmatrix} \psi_{\theta_1} e^{-i\omega t} \\ \psi_{\theta_2} e^{-i\omega t} \end{pmatrix} = 0\,,$$

which leads to the coupled equations,

$$\begin{aligned} \left(f\partial_r + \frac{f'}{4} + (D-4)\,\frac{f}{2r} - \left(\frac{\bar{\xi}\sqrt{f}}{r} - \frac{Q\sqrt{f}}{2r^{D-2}}\sqrt{\frac{D-2}{2\,(D-3)}}\right)\right)\psi_{\theta_1} &= i\omega\,\psi_{\theta_2}\,, \\ \left(f\partial_r + \frac{f'}{4} + (D-4)\,\frac{f}{2r} + \left(\frac{\bar{\xi}\sqrt{f}}{r} - \frac{Q\sqrt{f}}{2r^{D-2}}\sqrt{\frac{D-2}{2\,(D-3)}}\right)\right)\psi_{\theta_2} &= i\omega\,\psi_{\theta_1}\,. \end{aligned} \tag{6.23}$$

We can simplify the two above equations by writing,

$$\begin{aligned} \hat{\psi}_{\theta_1} &= r^{\frac{D-4}{2}} f^{1/4}\psi_{\theta_1} \\ \hat{\psi}_{\theta_2} &= r^{\frac{D-4}{2}} f^{1/4}\psi_{\theta_2}\,. \end{aligned} \tag{6.24}$$

Taking the radial derivatives of Eq.(6.24) and multiplying it with $r^{-(D-4)/2}\, f^{3/4}$ results in

$$\begin{aligned} r^{-\frac{D-4}{2}}\, f^{3/4}\partial_r\hat{\psi}_{\theta_1} &= \left(\frac{D-4}{2}\right)\frac{1}{r}f\psi_{\theta_1} + \frac{f'}{4}\psi_{\theta_1} + f\partial_r\psi_{\theta_1}\,, \\ r^{-\frac{D-4}{2}}\, f^{3/4}\partial_r\hat{\psi}_{\theta_2} &= \left(\frac{D-4}{2}\right)\frac{1}{r}f\psi_{\theta_2} + \frac{f'}{4}\psi_{\theta_2} + f\partial_r\psi_{\theta_1}\,. \end{aligned} \tag{6.25}$$

This leads to the coupled equations:

$$\begin{aligned} r^{-\frac{D-4}{2}}\, f^{3/4}\partial_r\hat{\psi}_{\theta_1} - \left(\frac{\bar{\xi}\sqrt{f}}{r} - \frac{q\sqrt{f}}{2r^{D-2}}\sqrt{\frac{D-2}{2\,(D-3)}}\right) r^{-\frac{D-4}{2}} f^{-1/4}\hat{\psi}_{\theta_1} &= i\omega\, r^{-\frac{D-4}{2}} f^{-1/4}\hat{\psi}_{\theta_2}\,, \\ r^{-\frac{D-4}{2}}\, f^{3/4}\partial_r\hat{\psi}_{\theta_2} + \left(\frac{\bar{\xi}\sqrt{f}}{r} - \frac{q\sqrt{f}}{2r^{D-2}}\sqrt{\frac{D-2}{2\,(D-3)}}\right) r^{-\frac{D-4}{2}} f^{-1/4}\hat{\psi}_{\theta_2} &= i\omega\, r^{-\frac{D-4}{2}} f^{-1/4}\hat{\psi}_{\theta_1}\,. \end{aligned} \tag{6.26}$$

Multiplying both equations by $r^{(D-4)/2} f^{1/4}$, to further simplify the above equations to get,

$$
\begin{aligned}
&f\partial_r\hat{\psi}_{\theta_1} - \left(\frac{\bar{\xi}\sqrt{f}}{r} - \frac{q\sqrt{f}}{2r^{D-2}}\sqrt{\frac{D-2}{2\,(D-3)}}\right)\hat{\psi}_{\theta_1} = i\omega\,\hat{\psi}_{\theta_2}\,,\\
&f\partial_r\hat{\psi}_{\theta_2} + \left(\frac{\bar{\xi}\sqrt{f}}{r} - \frac{q\sqrt{f}}{2r^{D-2}}\sqrt{\frac{D-2}{2\,(D-3)}}\right)\hat{\psi}_{\theta_2} = i\omega\,\hat{\psi}_{\theta_1}\,,
\end{aligned}
\tag{6.27}
$$

which can be compactly written as

$$
\begin{aligned}
&(f\partial_r - W)\,\hat{\psi}_{\theta_1} = i\omega\,\hat{\psi}_{\theta_2}\,,\\
&(f\partial_r + W)\,\hat{\psi}_{\theta_2} = i\omega\,\hat{\psi}_{\theta_1}\,.
\end{aligned}
\tag{6.28}
$$

The "superpotential" is found to be

$$
W = \left(\frac{\bar{\xi}\sqrt{f}}{r} - \frac{q\sqrt{f}}{2r^{D-2}}\sqrt{\frac{D-2}{2\,(D-3)}}\right)\,.
$$

The final decoupled equations are

$$
\begin{aligned}
&-\frac{d^2\hat{\psi}_{\theta_1}}{dr^2} + V_1\hat{\psi}_{\theta_1} = \omega^2\hat{\psi}_{\theta_1}\\
&-\frac{d^2\hat{\psi}_{\theta_2}}{dr^2} + V_2\hat{\psi}_{\theta_2} = \omega^2\hat{\psi}_{\theta_2}\,,
\end{aligned}
\tag{6.29}
$$

and finally the potential "V" can be computed from the "W" function as

$$
V_{1,2} = \pm f(r)\frac{dW}{dr} + W^2\,. \tag{6.30}
$$

Now that we know what the potential is, we are in a position to use the approximation methods developed in chapter 2 to calculate the QNFs for the TT-eigenmodes. With the WKB approximation method we use 3rd order and 6th order, whilst with the improved AIM we use 200 iterations to generate tables listing QNFs for three cases: $Q = 0.1 \times M$, $q = 0.5 \times M$, and $q = 1 \times M$. Our interest in the chosen values of Q is rooted in the fact that the only physically allowed values for Q are between $0 \times M$ and $1 \times M$ ($q \,\epsilon\, [0,1] \times M$). The case where $Q = 0$ reduces the problem to a Schwarzschild background, and the case $Q = 1 \times M$ is the extremal case.

4 Dimensions				
l	n	WKB 3rd order	WKB 6th order	AIM
0	0	0.3609-0.0949i	0.3625-0.0947i	0.3625-0.0947i
1	0	0.5649-0.0956i	0.5653-0.0956i	0.5653-0.0956i
1	1	0.5472-0.2910i	0.5480-0.2907i	0.5480-0.2907i
2	0	0.7672-0.0961i	0.7674-0.0961i	0.7673-0.0960i
2	1	0.7540-0.2904i	0.7544-0.2903i	0.7543-0.2903i
2	2	0.7307-0.4898i	0.7300-0.4908i	0.7299-0.4908i
3	0	0.9690-0.0963i	0.9691-0.0963i	0.9690-0.0963i
3	1	0.9586-0.2904i	0.9587-0.2904i	0.9587-0.2903i
3	2	0.9393-0.4879i	0.9388-0.4884i	0.9388-0.4884i
3	3	0.9133-0.6896i	0.9109-0.6928i	0.9108-0.6927i
4	0	1.1706-0.0965i	1.1707-0.0965i	1.1706-0.0965i
4	1	1.1620-0.2905i	1.1621-0.2905i	1.1620-0.2904i
4	2	1.1456-0.4870i	1.1453-0.4873i	1.1452-0.4872i
4	3	1.1230-0.6868i	1.1213-0.6885i	1.1212-0.6884i
4	4	1.0955-0.8898i	1.0913-0.8956i	1.0912-0.8956i
5	0	1.3721-0.0967i	1.3722-0.0966i	1.3721-0.0966i
5	1	1.3648-0.2906i	1.3648-0.2906i	1.3648-0.2906i
5	2	1.3506-0.4865i	1.3504-0.4867i	1.3503-0.4866i
5	3	1.3306-0.6851i	1.3294-0.6860i	1.3293-0.6860i
5	4	1.3060-0.8864i	1.3028-0.8898i	1.3027-0.8898i
5	5	1.2775-1.0904i	1.2715-1.0990i	1.2715-1.0990i

Table 6.1: *($n \leq l$, with $l = j - 3/2$) spin-3/2 field QNFs using the WKB and the AIM methods with $D = 4$.*

5 Dimensions				
l	n	WKB 3rd order	WKB 6th order	AIM
0	0	0.8230-0.2441i	0.8327-0.2458i	0.8326-0.2457i
1	0	1.1899-0.2456i	1.1930-0.2460i	1.1929-0.2460i
1	1	1.1102-0.7567i	1.1192-0.7550i	1.1191-0.7549i
2	0	1.5498-0.2465i	1.5511-0.2465i	1.5511-0.2465i
2	1	1.4894-0.7504i	1.4934-0.7496i	1.4933-0.7495i
2	2	1.3840-1.2775i	1.3834-1.2832i	1.3833-1.2831i
3	0	1.9076-0.2470i	1.9082-0.2470i	1.9082-0.2469i
3	1	1.8589-0.7479i	1.8609-0.7475i	1.8608-0.7475i
3	2	1.7703-1.2655i	1.7690-1.2683i	1.7924-1.2829i
3	3	1.6521-1.8007i	1.6391-1.8230i	1.6390-1.8229i
4	0	2.2645-0.2473i	2.2648-0.2473i	2.2648-0.2473i
4	1	2.2236-0.7468i	2.2247-0.7466i	2.2247-0.7466i
4	2	2.1474-1.2588i	2.1462-1.2603i	2.1461-1.2603i
4	3	2.0432-1.7855i	2.0329-1.7982i	2.0329-1.7982i
4	4	1.9168-2.3254i	1.8910-2.3698i	1.8910-2.3698i
5	0	2.6209-0.2476i	2.6211-0.2476i	2.6211-0.2475i
5	1	2.5857-0.7463i	2.5863-0.7462i	2.5863-0.7462i
5	2	2.5189-1.2547i	2.5178-1.2556i	2.5178-1.2555i
5	3	2.4259-1.7754i	2.4180-1.7831i	2.4180-1.7830i
5	4	2.3118-2.3081i	2.2907-2.3360i	2.2907-2.3359i
5	5	2.1794-2.8511i	2.1411-2.9210i	2.1410-2.9210i

Table 6.2: *($n \leq l$, with $l = j - 3/2$) spin-3/2 field QNFs using the WKB and the AIM methods with $D = 5$.*

6 Dimensions				
l	n	WKB 3rd order	WKB 6th order	AIM
0	0	1.2679-0.3824i	1.2887-0.3937i	1.2886-0.3936i
1	0	1.7447-0.3861i	1.7526-0.3889i	1.7538-0.3871i
1	1	1.5640-1.2013i	1.5932-1.2023i	1.5932-1.2022i
2	0	2.2081-0.3877i	2.2119-0.3882i	2.2120-0.3879i
2	1	2.0707-1.1865i	2.0850-1.1848i	2.0849-1.1848i
2	2	1.8276-2.0373i	1.8331-2.0490i	1.8331-2.0489i
3	0	2.6668-0.3885i	2.6687-0.3885i	2.6687-0.3885i
3	1	2.5558-1.1803i	2.5633-1.1788i	2.5633-1.1788i
3	2	2.3515-2.0086i	2.3526-2.0129i	2.3525-2.0129i
3	3	2.0759-2.8774i	2.0414-2.9300i	2.0414-2.9299i
4	0	3.1235-0.3889i	3.1246-0.3889i	3.1245-0.3889i
4	1	3.0301-1.1772i	3.0344-1.1763i	3.0343-1.1762i
4	2	2.8542-1.9924i	2.8537-1.9945i	2.8536-1.9944i
4	3	2.6114-2.8410i	2.5845-2.8703i	2.5845-2.8703i
4	4	2.3138-3.7206i	2.2343-3.8360i	2.2343-3.8360i
5	0	3.5792-0.3892i	3.5799-0.3892i	3.5798-0.3892i
5	1	3.4984-1.1755i	3.5010-1.1749i	3.5009-1.1748i
5	2	3.3439-1.9824i	3.3430-1.9836i	3.3429-1.9836i
5	3	3.1272-2.8169i	3.1066-2.8347i	3.1065-2.8346i
5	4	2.8586-3.6793i	2.7957-3.7513i	2.7957-3.7512i
5	5	2.5446-4.5664i	2.4187-4.7595i	2.4187-4.7595i

Table 6.3: *($n \leq l$, with $l = j - 3/2$) spin-3/2 field QNFs frequencies using the WKB and the AIM methods with $D = 6$.*

As we increase the number of dimensions, we increase the QNFs numbers for both the real and the imaginary parts. This increase is seen in all the approximation methods used. The 3rd order WKB QNFs values, however, increase faster than then QNFs values for the 6th order WKB and the AIM.

6.2.2 Non-TT eigenfunctions:

Unlike the TT eigenfunction the angular eigenfunction can be written as,

$$\Psi_{\theta_1} = \psi^1_\theta \otimes \bar{\nabla}_{\theta_i}\bar{\psi}_\lambda + \psi^2_\theta \otimes \bar{\gamma}_{\theta_i}\bar{\psi}_\lambda \,, \tag{6.31}$$

but we still retain the Weyl gauge, $\psi_t = 0$. The bi-spinors $\psi^1_{\underline{\theta}}$ and $\psi^2_{\underline{\theta}}$ are functions of only t and r. The $(D-2)$-sphere eigenspinor, $\bar{\psi}_\lambda$, has eigenvalue $i\bar{\lambda}$ where $\bar{\lambda} = j + (D-3)/2$.

Thus, the non-TT potential function is given by,

$$V = f(r)\frac{dW}{dr} + W^2 \,, \tag{6.32}$$

where

$$\begin{aligned} W = &\frac{(D-3)\sqrt{f}}{ABr}\left[\left(\frac{2}{D-2}\right)\left(\bar{\lambda}+C\right)AB + \left(\frac{D-2}{2}\right)\left(\bar{\lambda}+C-\bar{\lambda}f\right)\right] \\ &- \frac{1}{r}\left(\frac{D-4}{D-2}\right)\sqrt{f}\left(\bar{\lambda}+C\right) \,, \end{aligned} \tag{6.33}$$

and

$$\begin{aligned} A &= \frac{(D-2)}{2}\sqrt{f} - \bar{\lambda} + \frac{q}{2r^{D-3}}\sqrt{\frac{D-2}{2\,(D-3)}} \\ B &= \frac{(D-2)}{2}\sqrt{f} - \bar{\lambda} - \frac{q}{2r^{D-3}}\sqrt{\frac{D-2}{2\,(D-3)}} \\ C &= \frac{q}{2r^{D-3}}\sqrt{\frac{D-2}{2\,(D-3)}} \,. \end{aligned} \tag{6.34}$$

Our main focus is the behavior of the potential, and hence, the QNMs for higher dimensions (4 to 9). We will, however, start by doing an analysis of the results obtained for the $D = 4$ case and then move to the higher dimensional results.

The plots below represent the above potential function, for 4 dimensions, plotted for values of $l\,\epsilon\,[0,5]$:

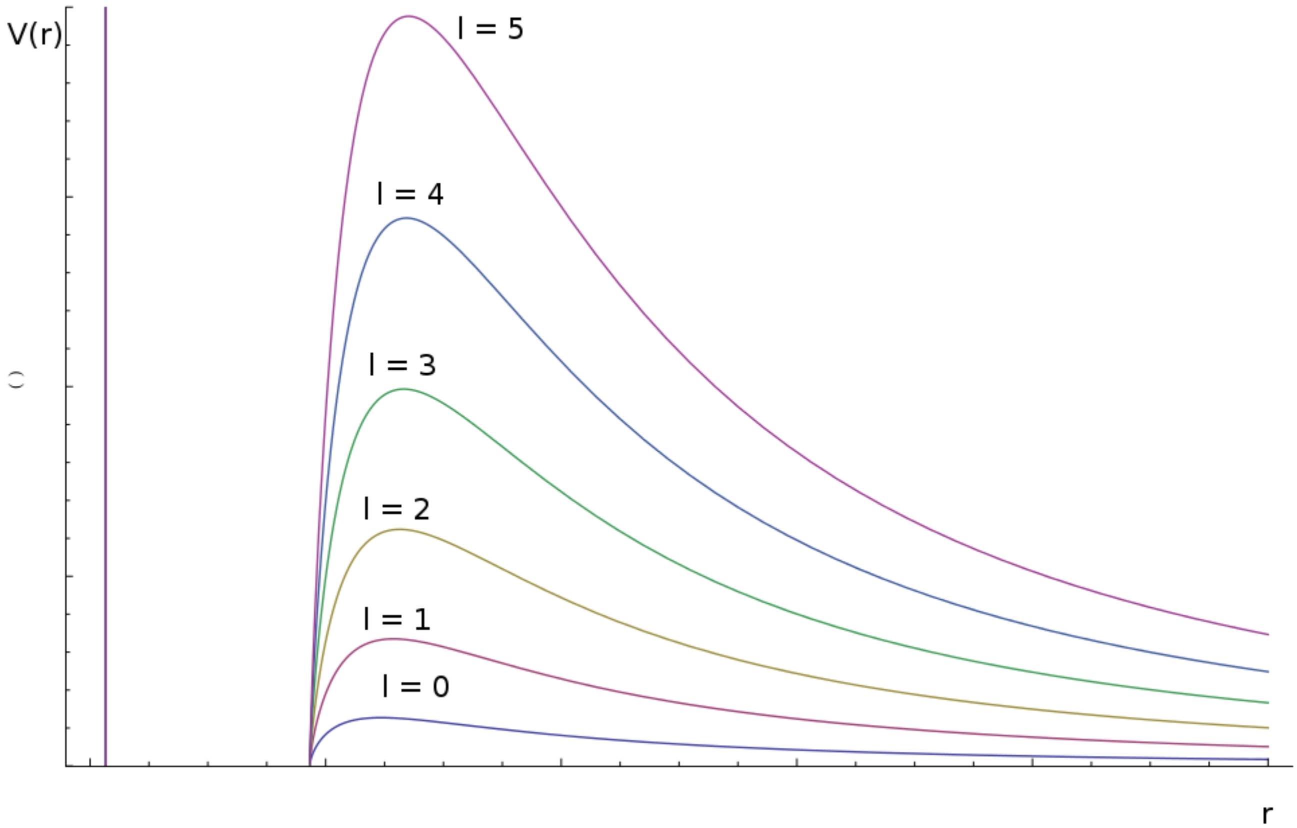

Figure 6.1: Potential function plot for $D = 4$ such that $l\,\epsilon\,[0,5]$.

The potential plots for $D = 5, .., 8$ are given in below:

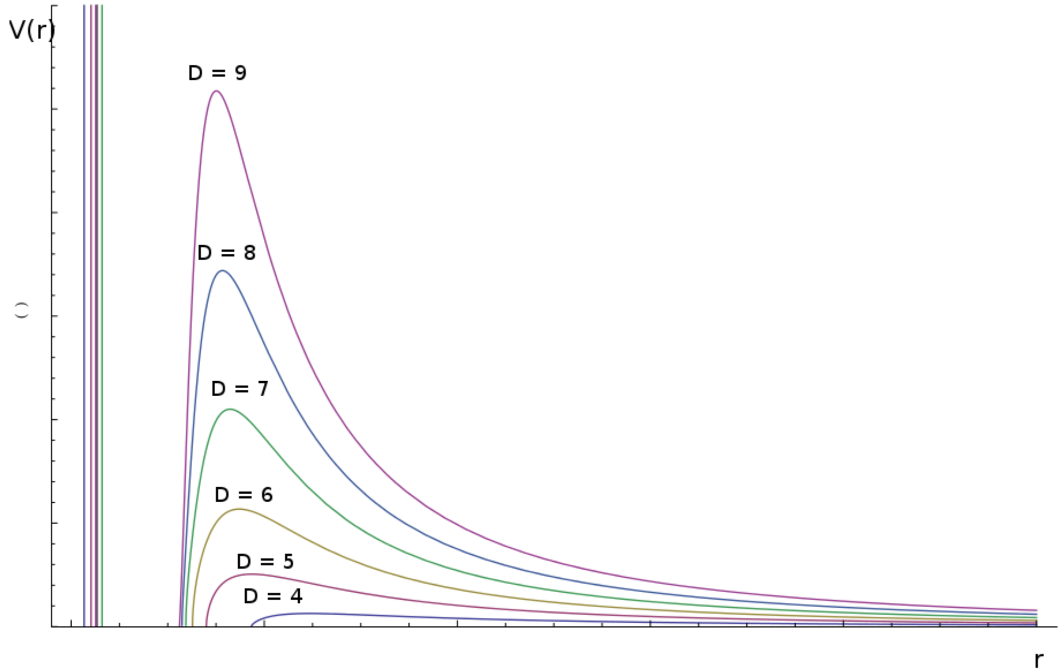

Figure 6.2: Potential function for $l = 0$ and $D \,\epsilon\, [4, 9]$.

These plots informs us that we are still within the region of the WKB, and thus, we used the WKB as well as AIM to produce the numbers for the QNFs of the spin-3/2 field in a D-dimensional Reissner-Nordstrøm black hole background. Below are the tables showing QNFs for the 3rd and 6th order WKB approximation method for $D = 4$ and $D = 5$ for the charge of the black hole is $Q = 0.1$:

4 Dimensions				
l	n	WKB 3rd order	WKB 6th order	AIM
0	0	0.3100-0.0902i	0.3125-0.0902i	0.1547-0.1870i
1	0	0.5308-0.0938i	0.5313-0.0938i	0.5313-0.0938i
1	1	0.5116-0.2860i	0.5127-0.2856i	0.5127-0.2856i
2	0	0.7359-0.0949i	0.7361-0.0949i	0.7361-0.0949i
2	1	0.7221-0.2872i	0.7225-0.2871i	0.7224-0.2870i
2	2	0.6974-0.4847i	0.6967-0.4858i	0.6967-0.4857i
3	0	0.9357-0.0954i	0.9358-0.0954i	0.9358-0.0954i
3	1	0.9248-0.2877i	0.9250-0.2877i	0.9249-0.2876i
3	2	0.9046-0.4837i	0.9041-0.4842i	0.9041-0.4841i
3	3	0.8775-0.6838i	0.8748-0.6873i	0.8748-0.6873i
4	0	1.1330-0.0957i	1.1331-0.0957i	1.1330-0.0956i
4	1	1.1240-0.2880i	1.1241-0.2880i	1.1240-0.2880i
4	2	1.1069-0.4830i	1.1066-0.4833i	1.1065-0.4832i
4	3	1.0833-0.6814i	1.0815-0.6833i	1.0814-0.6832i
4	4	1.0546-0.8831i	1.0501-0.8894i	1.0501-0.8894i
5	0	1.3289-0.0958i	1.3289-0.0958i	1.3289-0.0958i
5	1	1.3212-0.2882i	1.3213-0.2882i	1.3212-0.2882i
5	2	1.3064-0.4826i	1.3062-0.4828i	1.3061-0.4827i
5	3	1.2856-0.6797i	1.2843-0.6808i	1.2842-0.6807i
5	4	1.2599-0.8798i	1.2565-0.8835i	1.2564-0.8834i
5	5	1.2302-1.0825i	1.2239-1.0918i	1.2238-1.0918i

Table 6.4: , $Q = 0.1$, *($n \leq l$, with $l = j - 3/2$) spin-3/2 field QNF using the WKB and the AIM methods with $D = 4$*

5 Dimensions				
l	n	WKB 3rd order	WKB 6th order	AIM
0	0	0.6251-0.2151i	0.6553-0.2073i	0.5376-0.2286i
1	0	1.0666-0.2337i	1.0702-0.2337i	0.5680-0.3164i
1	1	0.9787-0.7226i	0.9878-0.7201i	0.2264-0.6065i
2	0	1.4616-0.2405i	1.4631-0.2404i	1.4682-0.2606i
2	1	1.3978-0.7329i	1.4036-0.7307i	1.1468-0.6769i
2	2	1.2862-1.2494i	1.2925-1.2474i	0.6274-0.6569i
3	0	1.8401-0.2437i	1.8407-0.2437i	1.6776-0.2944i
3	1	1.7895-0.7384i	1.7908-0.7382i	1.7645-0.7381i
3	2	1.6973-1.2502i	1.6920-1.2556i	1.6919-1.2555i
3	3	1.5740-1.7801i	1.5477-1.8168i	1.5477-1.8168i
4	0	2.2106-0.2456i	2.2109-0.2456i	2.1209-0.2693i
4	1	2.1684-0.7417i	2.1696-0.7414i	2.0175-0.7678i
4	2	2.0897-1.2505i	2.0889-1.2517i	2.0889-1.2516i
4	3	1.9820-1.7745i	1.9732-1.7856i	1.9731-1.7855i
4	4	1.8511-2.3119i	1.8290-2.3510i	1.8289-2.3509i
5	0	2.5763-0.2467i	2.5766-0.2467i	2.5100-0.2466i
5	1	2.5401-0.7438i	2.5408-0.7437i	2.5407-0.7436i
5	2	2.4714-1.2506i	2.4702-1.2516i	2.4701-1.2485i
5	3	2.3758-1.7701i	2.3669-1.7784i	2.3668-1.7660i
5	4	2.2582-2.3019i	2.2344-2.3322i	2.0234-2.1701i
5	5	2.1217-2.8440i	2.0777-2.9212i	2.0777-2.8859i

Table 6.5: , $Q = 0.1$, *($n \leq l$, with $l = j - 3/2$) spin-3/2 QNF using the WKB and the AIM methods in a 5-dimensional Reissner-Nordstrøm black hole background.*

6 Dimensions				
l	n	WKB 3rd order	WKB 6th order	AIM
0	0	0.9376-0.3560i	0.9073-0.3433i	0.9072-0.3432i
1	0	1.5058-0.3601i	1.5177-0.3535i	1.5176-0.3534i
1	1	1.3047-1.1246i	1.3428-1.0710i	1.3428-1.0710i
2	0	2.0248-0.3706i	2.0289-0.3696i	2.0289-0.3695i
2	1	1.8805-1.1350i	1.8967-1.1247i	1.8966-1.1247i
2	2	1.6222-1.9527i	1.6270-1.9385i	1.6269-1.9385i
3	0	2.5198-0.3770i	2.5216-0.3767i	0.5474-0.7188i
3	1	2.4055-1.1459i	2.4129-1.1426i	2.0440-0.9242i
3	2	2.1941-1.9513i	2.1938-1.9504i	2.0989-1.9276i
3	3	1.9072-2.7986i	1.8668-2.8409i	0.4801-0.7223i
4	0	3.0021-0.3810i	3.0031-0.3809i	0.7229-0.8154i
4	1	2.9067-1.1534i	2.9108-1.1519i	1.9227-0.9255i
4	2	2.7266-1.9528i	2.7252-1.9533i	1.5407-0.9786i
4	3	2.4771-2.7860i	2.4475-2.8121i	0.9460-1.0251i
4	4	2.1705-3.6514i	2.0843-3.7619i	0.5253-0.9348i
5	0	3.4769-0.3836i	3.4775-0.3836i	3.4774-0.3835i
5	1	3.3946-1.1586i	3.3971-1.1578i	3.3970-1.1578i
5	2	3.2373-1.9544i	3.2357-1.9550i	3.2357-1.9550i
5	3	3.0160-2.7779i	2.9937-2.7945i	2.8326-2.6168i
5	4	2.7412-3.6298i	2.6745-3.7003i	2.6744-3.7003i
5	5	2.4194-4.5074i	2.2861-4.6996i	2.2860-4.6995i

Table 6.6: $Q = 0.1$,*($n \leq l$, with $l = j - 3/2$) spin-3/2 field QNF using the WKB and the AIM methods with $D = 6$*

$Q = 0.5$

4 Dimensions				
l	n	WKB 3rd order	WKB 6th order	AIM
0	0	0.3178-0.0908i	0.3202-0.0906i	0.1507-0.1558i
1	0	0.5407-0.0944i	0.5412-0.0943i	0.5411-0.0943i
1	1	0.5220-0.2874i	0.5230-0.2871i	0.5230-0.2870i
2	0	0.7479-0.0954i	0.7481-0.0954i	0.7480-0.0954i
2	1	0.7343-0.2885i	0.7347-0.2885i	0.7346-0.2884i
2	2	0.7102-0.4869i	0.7095-0.4879i	0.7094-0.4879i
3	0	0.9498-0.0959i	0.9498-0.0959i	0.9498-0.0958i
3	1	0.9390-0.2891i	0.9392-0.2890i	0.9391-0.2890i
3	2	0.9192-0.4858i	0.9187-0.4863i	0.9186-0.4863i
3	3	0.8925-0.6868i	0.8900-0.6901i	0.8899-0.6901i
4	0	1.1491-0.0961i	1.1491-0.0961i	1.1491-0.0961i
4	1	1.1402-0.2893i	1.1403-0.2893i	1.1402-0.2893i
4	2	1.1234-0.4851i	1.1230-0.4854i	1.1230-0.4853i
4	3	1.1002-0.6843i	1.0984-0.6860i	1.0983-0.6860i
4	4	1.0720-0.8867i	1.0676-0.8928i	1.0675-0.8928i
5	0	1.3470-0.0963i	1.3470-0.0963i	1.3469-0.0962i
5	1	1.3394-0.2895i	1.3394-0.2895i	1.3394-0.2894i
5	2	1.3248-0.4846i	1.3246-0.4848i	1.3245-0.4847i
5	3	1.3043-0.6825i	1.3031-0.6835i	1.3030-0.6835i
5	4	1.2790-0.8833i	1.2757-0.8869i	1.2756-0.8868i
5	5	1.2498-1.0867i	1.2436-1.0958i	1.2435-1.0957i

Table 6.7: $Q = 0.5$, *($n \leq l$, with $l = j - 3/2$) spin-3/2 QNF using the WKB and the AIM methods with $D = 4$*

5 Dimensions				
l	n	WKB 3rd order	WKB 6th order	AIM
0	0	0.6333-0.2115i	0.6091-0.2538i	0.2956-0.2936i
1	0	1.0746-0.2333i	1.0779-0.2336i	0.2631-0.3620i
1	1	0.9909-0.7210i	1.0020-0.7175i	0.8549-0.6573i
2	0	1.4703-0.2404i	1.4713-0.2404i	0.6397-0.4230i
2	1	1.4080-0.7325i	1.4077-0.7335i	1.1063-0.7218i
2	2	1.2993-1.2485i	1.2782-1.2727i	0.6473-0.7106i
3	0	1.8496-0.2438i	1.8503-0.2437i	1.8503-0.2437i
3	1	1.7997-0.7384i	1.8025-0.7376i	1.2942-0.6409i
3	2	1.7090-1.2500i	1.7115-1.2496i	1.2991-0.9675i
3	3	1.5879-1.7796i	1.5869-1.7871i	1.1159-1.1976i
4	0	2.2206-0.2456i	2.2210-0.2456i	2.2210-0.2455i
4	1	2.1790-0.7418i	2.1804-0.7414i	2.1804-0.7414i
4	2	2.1012-1.2506i	2.1017-1.2509i	2.1017-1.2509i
4	3	1.9950-1.7744i	1.9908-1.7812i	1.9908-1.7812i
4	4	1.8659-2.3115i	1.8560-2.3351i	1.8559-2.3350i
5	0	2.5870-0.2467i	2.5872-0.2467i	2.5872-0.2467i
5	1	2.5511-0.7439i	2.5519-0.7437i	2.5519-0.7437i
5	2	2.4832-1.2507i	2.4828-1.2513i	2.4827-1.2512i
5	3	2.3885-1.7701i	2.3831-1.7758i	2.3831-1.7758i
5	4	2.2723-2.3017i	2.2582-2.3221i	2.2581-2.3221i
5	5	2.1374-2.8436i	2.1143-2.8920i	2.1142-2.8920i

Table 6.8: $Q = 0.5$, *($n \leq l$, with $l = j - 3/2$) spin-3/2 field QNF using the WKB and the AIM methods in a 5-dimensional Reissner-Nordstrøm black hole background.*

6 Dimensions				
l	n	WKB 3rd order	WKB 6th order	AIM
0	0	0.9309-0.3432i	0.9291-0.3008i	0.5439-0.3496i
1	0	1.5106-0.3567i	1.5260-0.3527i	1.5260-0.3526i
1	1	1.3118-1.1132i	1.3724-1.0698i	1.3723-1.0698i
2	0	2.0317-0.3696i	2.0358-0.3692i	0.4694-0.5972i
2	1	1.8902-1.1317i	1.9059-1.1263i	1.1867-1.0917i
2	2	1.6376-1.9462i	1.6444-1.9501i	1.6443-1.9501i
3	0	2.5277-0.3766i	2.5295-0.3764i	0.5064-0.6555i
3	1	2.4150-1.1445i	2.4222-1.1422i	2.0059-1.0306i
3	2	2.2071-1.9489i	2.2064-1.9516i	2.2064-1.9516i
3	3	1.9254-2.7944i	1.8861-2.8460i	1.8254-2.7281i
4	0	3.0106-0.3808i	3.0116-0.3807i	3.0115-0.3807i
4	1	2.9162-1.1528i	2.9201-1.1516i	2.9201-1.1515i
4	2	2.7382-1.9517i	2.7365-1.9533i	2.7365-1.9532i
4	3	2.4921-2.7842i	2.4620-2.8132i	2.4620-2.8131i
4	4	2.1898-3.6483i	2.1038-3.7651i	2.1038-3.7650i
5	0	3.4858-0.3835i	3.4864-0.3835i	3.4863-0.3834i
5	1	3.4042-1.1583i	3.4066-1.1576i	3.4066-1.1576i
5	2	3.2483-1.9538i	3.2466-1.9548i	3.2466-1.9548i
5	3	3.0293-2.7770i	3.0068-2.7946i	3.0068-2.7945i
5	4	2.7575-3.6283i	2.6907-3.7009i	2.6907-3.7008i
5	5	2.4395-4.5049i	2.3066-4.7007i	2.3066-4.7007i

Table 6.9: $Q = 0.5$, *($n \leq l$, with $l = j - 3/2$) spin-3/2 field QNF using the WKB and the AIM methods with $D = 6$*

The following tables will be based on $Q = 1$:

4 Dimensions				
l	n	WKB 3rd order	WKB 6th order	AIM
0	0	0.9208-0.3218i	1.0264-0.1870i	0.9817-0.1697i
1	0	1.5181-0.3519i	1.5351-0.3551i	0.6349-0.4507i
1	1	1.3246-1.0974i	1.4037-1.1002i	1.1376-0.8516i
2	0	2.0419-0.3680i	2.0453-0.3687i	1.8639-0.5441i
2	1	1.9051-1.1267i	1.9168-1.1306i	1.7011-1.1178i
2	2	1.6620-1.9368i	1.6627-1.9777i	1.6627-1.9776i
3	0	2.5392-0.3757i	2.5410-0.3758i	2.5288-0.4434i
3	1	2.4293-1.1419i	2.4355-1.1411i	1.6816-0.9158i
3	2	2.2270-1.9442i	2.2241-1.9529i	1.0153-0.9447i
3	3	1.9538-2.7866i	1.9122-2.8541i	0.6924-1.0500i
4	0	3.0232-0.3802i	3.0242-0.3802i	1.8746-0.7060i
4	1	2.9305-1.1510i	2.9342-1.1502i	2.8359-1.1486i
4	2	2.7561-1.9486i	2.7538-1.9515i	2.0300-1.4196i
4	3	2.5155-2.7793i	2.4846-2.8118i	1.3734-1.4384i
4	4	2.2205-3.6408i	2.1343-3.7647i	0.9257-1.8031i
5	0	3.4992-0.3831i	3.4998-0.3830i	1.1775-1.0020i
5	1	3.4189-1.1569i	3.4212-1.1563i	2.8697-1.1363i
5	2	3.2655-1.9514i	3.2637-1.9528i	3.2636-1.9528i
5	3	3.0504-2.7733i	3.0277-2.7919i	3.0277-2.7919i
5	4	2.7838-3.6228i	2.7173-3.6974i	2.7172-3.6974i
5	5	2.4721-4.4970i	2.3406-4.6959i	2.3405-4.6958i

Table 6.10: $Q = 1$, *($n \leq l$, with $l = j - 3/2$) spin-3/2 field QNF using the WKB and the AIM methods with $D = 4$*

6 Dimensions				
l	n	WKB 3rd order	WKB 6th order	AIM
0	0	0.9208-0.3218i	1.0264-0.1870i	0.9817-0.1697i
1	0	1.5181-0.3519i	1.5351-0.3551i	0.6349-0.4507i
1	1	1.3246-1.0974i	1.4037-1.1002i	1.1376-0.8516i
2	0	2.0419-0.3680i	2.0453-0.3687i	1.8639-0.5441i
2	1	1.9051-1.1267i	1.9168-1.1306i	1.7011-1.1178i
2	2	1.6620-1.9368i	1.6627-1.9777i	1.6627-1.9776i
3	0	2.5392-0.3757i	2.5410-0.3758i	2.5288-0.4434i
3	1	2.4293-1.1419i	2.4355-1.1411i	1.6816-0.9158i
3	2	2.2270-1.9442i	2.2241-1.9529i	1.0153-0.9447i
3	3	1.9538-2.7866i	1.9122-2.8541i	0.6924-1.0500i
4	0	3.0232-0.3802i	3.0242-0.3802i	1.8746-0.7060i
4	1	2.9305-1.1510i	2.9342-1.1502i	2.8359-1.1486i
4	2	2.7561-1.9486i	2.7538-1.9515i	2.0300-1.4196i
4	3	2.5155-2.7793i	2.4846-2.8118i	1.3734-1.4384i
4	4	2.2205-3.6408i	2.1343-3.7647i	0.9257-1.8031i
5	0	3.4992-0.3831i	3.4998-0.3830i	1.1775-1.0020i
5	1	3.4189-1.1569i	3.4212-1.1563i	2.8697-1.1363i
5	2	3.2655-1.9514i	3.2637-1.9528i	3.2636-1.9528i
5	3	3.0504-2.7733i	3.0277-2.7919i	3.0277-2.7919i
5	4	2.7838-3.6228i	2.7173-3.6974i	2.7172-3.6974i
5	5	2.4721-4.4970i	2.3406-4.6959i	2.3405-4.6958i

Table 6.11: $Q = 1$, *($n \leq l$, with $l = j - 3/2$) spin-3/2 field QNF using the WKB and the AIM methods with $D = 6$.*

Figure 6.3 compares the QNFs obtained in this work, those in the D-dimensional Reissner-Nordstr$\o$m background, and for a D-dimensional Schwarzschild background [31], for spin-3/2 field.

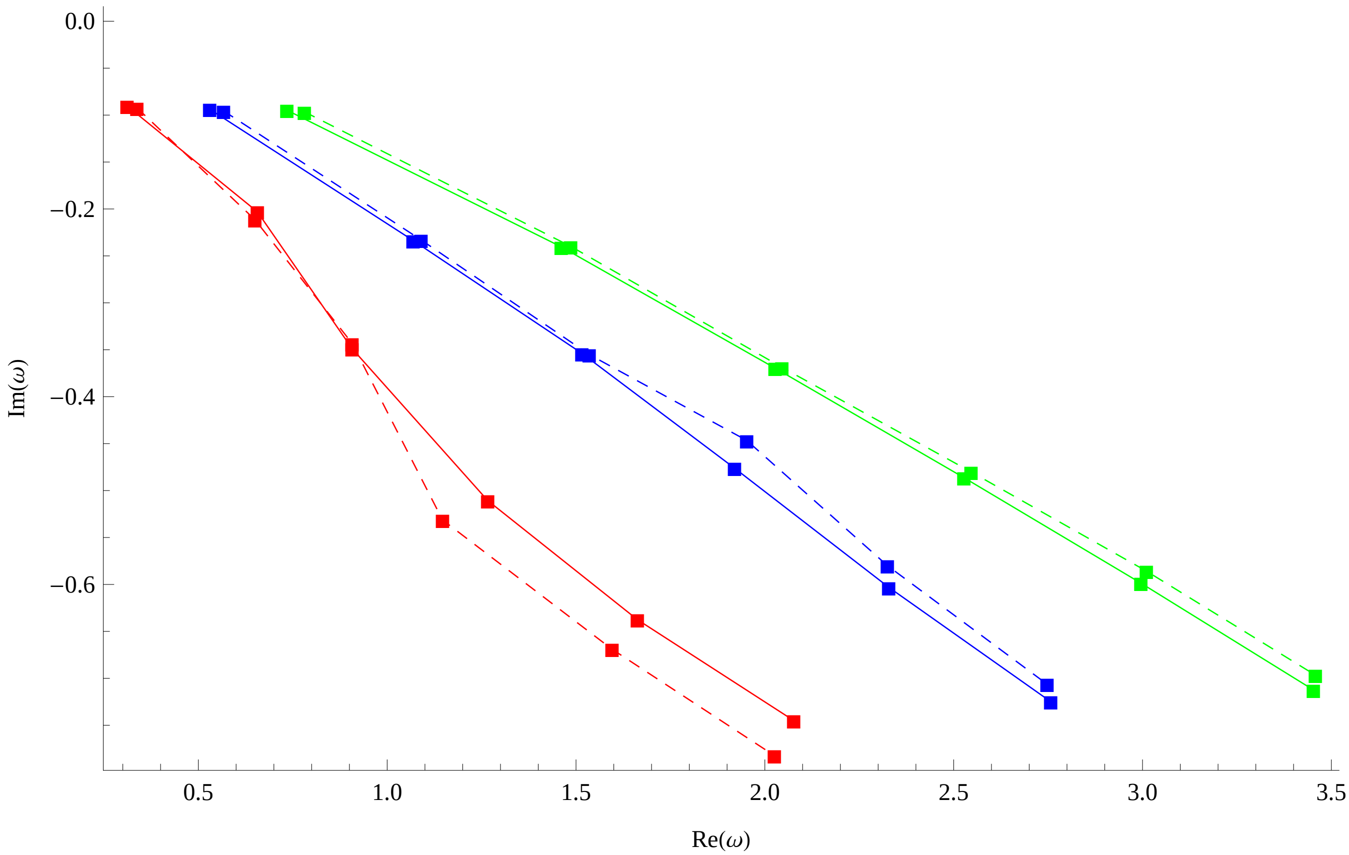

Figure 6.3: *Comparison between the Schwarzschild (solid lines) and Reissner-Nordstr$\o$m (dashed lines) QNMs for different l*

For higher modes (the green line) there is close agreement between the Schwarzschild case and the Reissner-Nordstr$\o$m case. We observe few disagreements as we go to low lying modes. This disagreement becomes very clear where we have a dip (the red line) in the Schwarzschild case and a bump (blue line) in the Reissner-Nordstr$\o$m. We cannot, at this point, explain the dip and the bump, perhaps this calls for a deeper study.

Chapter 7

Concluding Remarks

We started with a review of the scalar field in a Schwarzschild black hole background (the simplest case) in chapter 4 as to demonstrate the idea of computing QNMs. We realised that the equation(s) that needed to be solved in order to compute QNMs could not be solved analytically and this motivated us to look for numerical methods we can employ to solve these equations. It turned out that the equation we needed to solve to get the QNMs was the radial part of the equation(s) of motion. The structure of this equation

$$\frac{d\Psi}{dx^2} + \left(\omega^2 - V(x)\right)\Psi = 0\,, \tag{7.1}$$

lead us to using two approximation methods; the WKB and AIM. These methods are used to solve second order differential equations like the one above. With the use of these methods we computed the QNFs for the scalar field in a Schwarzschild black hole background, listed in chapter 6. We compared these results with the ones in literature in ref. [1] and the 3rd order WKB matched the results as they also used 3rd order WKB. We refined the results by using the 3rd order WKB results to seed our 6th order WKB and AIM in order to refine the precision of these QNFs.

Given that we managed to reproduce the literature QNFs for the scalar field, we then proceeded to computing the QNFs for the spin-3/2 field described by the Rarita-Schwinger equation. In chapter 5 we introduced the theory behind the spin-3/2 field in the D-dimensional black hole background. following the same procedure as the scalar field, we solved the Rarita-schwinger equation and the radial part of the equation gave us the QNFs. With the use of the approximation methods, we computed the QNFs for this set-up and the results are listed in chapter 6.

We computed the QNFs for three cases; the $Q = 0.1\,,\ Q = 0.5\,,\ Q = 1\,.$ The case for $Q = 0$ reduces the background from Reissner-Nordstr$\not{o}$m to D-dimensional Schwarzschild background. Following the QNMs for a spin-3/2 in this case have been computed in ref. [2]. Thus, since this case has been studied thoroughly before we decided not to include it in this work. In fact, this work follows from turning the charge on in the Schwarzscild case. There is a strong agreement between the 6th order WKB numbers and improved AIM numbers.

Bibliography

[1] S. Iyer and C. M. Will, "Black-hole normal modes: A wkb approach. i. foundations and application of a higher-order wkb analysis of potential-barrier scattering," *Phys. Rev. D*, vol. 35, pp. 3621–3631, 1987.

[2] H. T. Cho, A. S. Cornell, J. Doukas, T. R. Huang, and W. Naylor, "A New Approach to Black Hole Quasinormal Modes: A Review of the Asymptotic Iteration Method," *Adv. Math. Phys.*, vol. 2012, p. 281705, 2012.

[3] W. Rarita and J. Schwinger, "On a theory of particles with half-integral spin," *Phys. Rev.*, vol. 60, pp. 61–61, Jul 1941.

[4] M. Fierz and W. Pauli, "On relativistic wave equations for particles of arbitrary spin in an electromagnetic field," *Proceedings of the Royal Society of London. Series A, Mathematical and Physical Sciences*, vol. 173, no. 953, pp. 211–232, 1939.

[5] G. Velo and D. Zwanziger, "Propagation and quantization of rarita-schwinger waves in an external electromagnetic potential," *Phys. Rev.*, vol. 186, pp. 1337–1341, Oct 1969.

[6] R. Kerr and A. Schild, "Einstein field equations.," 1965.

[7] K. Schwarzschild, "On the Gravitational Field of a Mass Point According to Einstein's Theory," *Proceedings of the Prussian Academy of Science*, vol. 423.

[8] H. Reissner, "ber die Eigengravitation des elektrischen Feldes nach der Einsteinschen Theorie," *Annalen der Physik*, vol. 355.

[9] G. Nordstrm, "On the energy of the gravitational field in Einstein's theory," *Proc. Kon. Ned. Akad. Wet.*, vol. 20.

[10] G. Kang, "Quantization of scalar field in the presence of imaginary frequency modes," pp. 282–286, 1996. [Astrophys. Space Sci. Libr.211,282(1997)].

[11] P. A. M. Dirac, "Relativistic wave equations," *Proceedings of the Royal Society of London. Series A, Mathematical and Physical Sciences*, vol. 155, no. 886, pp. 447–459, 1936.

[12] H. Ciftci, R. L. Hall, N. Saad, and E. Dogu, "Physical applications of second-order linear differential equations that admit polynomial solutions," *arXiv preprint arXiv:1009.0464*, 2010.

[13] J. S. Geronimo, "Wkb and turning point theory for second order difference equations: external fields and strong asymptotics for orthogonal polynomials," *arXiv preprint arXiv:0905.1684*, 2009.

[14] M. Saleh, B. T. Bouetou, and T. C. Kofane, "Quasinormal modes and Hawking radiation of a Reissner-Nordstroem black hole surrounded by quintessence," *Astrophys. Space Sci.*, vol. 333, pp. 449–455, 2011.

[15] J. Li, K. Lin, and N. Yang, "Nonlinear electromagnetic quasinormal modes and hawking radiation of a regular black hole with magnetic charge," *The European Physical Journal C*, vol. 75, no. 3, p. 131, 2015.

[16] Z. Nouredine, *Quantum Mechanics Concepts and Applications*. Wiley, 2009.

[17] B. Schutz and C. M. Will, "Black hole normal modes: A semianalytic approach," vol. 291, 03 1985.

[18] R. A. Konoplya, "Quasinormal behavior of the d-dimensional schwarzschild black hole and the higher order wkb approach," *Phys. Rev. D*, vol. 68, p. 024018, Jul 2003.

[19] B. Champion, R. L. Hall, and N. Saad, "Asymptotic Iteration Method for singular potentials," *[arXiv:0802.2072v1]*, 14 Feb 2008.

[20] O. BAYRAK, I. BOZTOSUN, and H. CIFTCI, "Exact Analytical Solutions to the Kratzer Potential by the Asymptotic Iteration Method," *Wiley InterScience*, vol. 2006, 22 September 2006.

[21] A. Einstein, "On the Electrodynamics of Moving Bodies," *Annalen der Physik*, vol. 17, pp. 891 – 921, 1905.

[22] L. Susskind and J. Uglum, "String physics and black holes," *Nucl. Phys. Proc. Suppl.*, vol. 45BC, pp. 115–134, 1996.

[23] S. W. Hawking, "The Information Paradox for Black Holes," 2015.

[24] J. Noble and U. D. Jentschura, "Dirac hamiltonian and reissner-nordström metric: Coulomb interaction in curved space-time," *Physical Review A*, vol. 93, no. 3, p. 032108, 2016.

[25] M. Cavaglia, "Black hole and brane production in TeV gravity: A Review," *Int. J. Mod. Phys.*, vol. A18, pp. 1843–1882, 2003.

[26] P. P. Avelino, A. J. S. Hamilton, C. A. R. Herdeiro, and M. Zilhao, "Mass inflation in a D dimensional Reissner-Nordstrom black hole: a hierarchy of particle accelerators ?," *Phys. Rev.*, vol. D84, p. 024019, 2011.

[27] J. Yepez, "Einstein's vierbein field theory of curved space," 2011.

[28] M. Saleh, B. T. Bouetou, and T. C. Kofane, "Quasinormal modes of a quantum-corrected schwarzschild black hole: gravitational and dirac perturbations," *Astrophysics and Space Science*, vol. 361, no. 4, p. 137, 2016.

[29] H. T. Cho, "Dirac quasinormal modes in Schwarzschild black hole space-times," *Phys. Rev.*, vol. D68, p. 024003, 2003.

[30] S. Deser and A. Waldron, "(dis)continuities of massless limits in spin-3/2-mediated interactions and cosmological supergravity," *Physics Letters B*, vol. 501, no. 12, pp. 134 – 139, 2001.

[31] C. H. Chen, H. T. Cho, A. S. Cornell, and G. Harmsen, "Spin- 3/2 fields in *D*-dimensional Schwarzschild black hole spacetimes," *Phys. Rev.*, vol. D94, no. 4, p. 044052, 2016.

[32] K. G. Savvidy, "Quantum electrodynamics of spin 3/2," *[arXiv:1005.3455v1]*, p. 18, 2010.

[33] R. Camporesi and A. Higuchi *Journal of Geometry and Physics*, vol. 20, p. 1, 1996.

Appendix A

Christoffel Symbols

The Christoffel symbols are given by the equation,

$$\Gamma^{\alpha}_{\mu\nu} = \frac{1}{2}\, g^{\alpha\rho}\left\{\partial_\mu g_{\nu\rho} + \partial_\nu g_{\rho\mu} - \partial_\rho g_{\mu\nu}\right\} \tag{A.1}$$

Noting that for $\alpha \neq \rho$, $g^{\alpha\rho} = 0$, and thus $\Gamma^{\alpha}_{\mu\nu} = 0$. So, only terms with $\alpha = \rho$ contribute to the Christoffel symbol,
taking

$$g_{\mu\nu} = \mathrm{diag}\left(-f(r),\, f(r)^{-1},\, r^2,\, r^2\sin^2\theta\right)\,,$$

noting that $g_{\mu\nu}$ is general at this point.

<u>**First we let** $\alpha = \rho = 0 = t$</u>

$$\begin{aligned}\Gamma^{t}_{\mu\nu} &= \frac{1}{2}\, g^{tt}\left\{\partial_\mu g_{\nu t} + \partial_\nu g_{t\mu} - \partial_t g_{\mu\nu}\right\}\\ &= \frac{1}{2}\, g^{tt}\left\{\partial_\mu g_{\nu t} + \partial_\nu g_{t\mu}\right\}\\ &= \frac{1}{2}\,(-f)^{-1}\left\{\partial_\mu g_{\nu t} + \partial_\nu g_{t\mu}\right\}\end{aligned} \tag{A.2}$$

there only exists three cases for the above equation; $\mu = \nu = t$, $\mu \neq \nu = t$, and $\nu \neq \mu = t$. We will start with the simple case;

<u>$\mu = \nu = t$:</u>

$$\begin{aligned}\Gamma^{t}_{tt} &= \frac{1}{2}\,(-f)^{-1}\left\{\partial_t g_{tt} + \partial_t g_{tt}\right\}\\ &= 0\end{aligned} \tag{A.3}$$

this is true because our metric does not depend on time.

<u>$\mu \neq \nu = r$</u>

$$\begin{aligned}\Gamma^{t}_{\mu r} &= \frac{1}{2}\, g^{tt}\left\{\partial_\mu g_{rt} + \partial_r g_{t\mu} - \partial_t g_{\mu r}\right\}\\ &= \frac{1}{2}\,(-f)^{-1}\left\{\partial_r g_{t\mu}\right\}\end{aligned} \tag{A.4}$$

$$\Rightarrow \Gamma^t_{tr} = \frac{1}{2}\,(-f)^{-1}\{\partial_r g_{tt}\} \\ = \frac{1}{2}\,\frac{f'}{f} \tag{A.5}$$

and we know that Christoffel symbols are symmetric in their lower indeces and thus,

$$\Gamma^t_{tr} = \Gamma^t_{rt} = \frac{1}{2}\,\frac{f'}{f}\,. \tag{A.6}$$

<u>**Secondly, we let** $\rho = \alpha = r$:</u>

$$\begin{aligned}\Gamma^r_{\mu\nu} &= \frac{1}{2}\,g^{rr}\{\partial_\mu g_{\nu r} + \partial_\nu g_{r\mu} - \partial_r g_{\mu\nu}\} \\ &= \frac{1}{2}\,(f)\{\partial_\mu g_{\nu r} + \partial_\nu g_{r\mu} - \partial_r g_{\mu\nu}\}\end{aligned} \tag{A.7}$$

we will start with $\mu = \nu$

$$\Gamma^r_{\mu\mu} = \frac{1}{2}\,(f)\{\partial_\mu g_{\mu r} + \partial_\mu g_{r\mu} - \partial_r g_{\mu\mu}\} \tag{A.8}$$

<u>$\mu = t$:</u>

$$\begin{aligned}\Gamma^r_{tt} &= \frac{1}{2}\,(f)\{\partial_t g_{tr} + \partial_t g_{rt} - \partial_r g_{tt}\} \\ &= \frac{1}{2}\,(f)\{-\partial_r(-f)\} \\ &= -\frac{f\,f'}{2}\,.\end{aligned} \tag{A.9}$$

<u>$\mu = r$:</u>

$$\begin{aligned}\Gamma^r_{rr} &= \frac{1}{2}\,(f)\{\partial_r g_{rr} + \partial_r g_{rr} - \partial_r g_{rr}\} \\ &= \frac{1}{2}\,(f)\{\partial_r g_{rr}\} \\ &= -\frac{1}{2}\,f\,f^{-2}f' \\ &= -\frac{f'}{2\,f}\,.\end{aligned} \tag{A.10}$$

<u>$\mu = \theta$:</u>

$$\begin{aligned}\Gamma^r_{\theta\theta} &= \frac{1}{2}\,f\ \{\partial_\theta g_{\theta r} + \partial_\theta g_{r\theta} - \partial_r g_{\theta\theta}\} \\ &= \frac{1}{2}\,f\ \{-\partial_r g_{\theta\theta}\} \\ &= -\frac{2}{2}\,f\,r \\ &= -f\,r\,.\end{aligned} \tag{A.11}$$

$\underline{\mu = \phi :}$

$$\begin{aligned}
\Gamma^{r}_{\phi\phi} &= \frac{1}{2}\, f\ \{\partial_\phi g_{\phi r} + \partial_\phi g_{r\phi} - \partial_r g_{\phi\phi}\} \\
&= \frac{1}{2}\, f\ \{-\partial_r g_{\phi\phi}\} \\
&= \frac{1}{2}\, f\ \left\{-2r\sin^2\theta\right\} \\
&= -f\, r\sin^2\theta\,.
\end{aligned} \tag{A.12}$$

$\underline{\mu \neq \nu :}$

$$\Gamma^{r}_{\mu\nu} = \frac{1}{2}\, f\ \{\partial_\mu g_{\nu r} + \partial_\nu g_{r\mu} - \partial_r g_{\mu\nu}\} = 0 \tag{A.13}$$

This is true based on the listed facts:

- $g_{\mu\nu}$ is time independent
- $g_{\mu\nu}$ is ϕ independent and,
- $\mu \neq \nu$.

Third case is $\alpha = \rho = \theta$:

$$\Gamma^{\theta}_{\mu\nu} = \frac{1}{2}\, r^{-2}\ \{\partial_\mu g_{\nu\theta} + \partial_\nu g_{\theta\mu} - \partial_\theta g_{\mu\nu}\} \tag{A.14}$$

$\underline{\mu = \nu}$:
In this case, only $\mu = \nu = \phi$ will be contributing:

$$\begin{aligned}
\Gamma^{\theta}_{\phi\phi} &= \frac{1}{2}\, r^{-2}\ \{\partial_\phi g_{\phi\theta} + \partial_\phi g_{\theta\phi} - \partial_\theta g_{\phi\phi}\} \\
&= \frac{1}{2}\, r^{-2}\ \{-\partial_\theta g_{\phi\phi}\} \\
&= \frac{1}{2}\, r^{-2}\ \left\{-2r^2\sin\theta\cos\theta\right\} \\
&= -\sin\theta\cos\theta.
\end{aligned} \tag{A.15}$$

$\underline{\mu \neq \nu :}$

$$\Gamma^{\theta}_{\mu\nu} = \frac{1}{2}\, r^{-2}\ \{\partial_\mu g_{\nu\theta} + \partial_\nu g_{\theta\mu} - \partial_\theta g_{\mu\nu}\} = 0 \tag{A.16}$$

for $\mu = t$ and $\nu \neq \mu$. For $\mu = r$ and $\mu \neq \nu$ we get

$$\begin{aligned}
\Gamma^{\theta}_{r\nu} &= \frac{1}{2}\, r^{-2}\ \{\partial_r g_{\nu\theta} + \partial_\nu g_{\theta r} - \partial_\theta g_{r\nu}\} \\
&= \frac{1}{2}\, r^{-2}\ \{\partial_r g_{\nu\theta}\}
\end{aligned} \tag{A.17}$$

$$
\begin{aligned}
\Rightarrow \Gamma^{\theta}_{r\theta} &= \frac{1}{2}\, r^{-2}\,(2r) \\
&= \frac{1}{r} \\
&= \Gamma^{\theta}_{\theta r}\,.
\end{aligned} \tag{A.18}
$$

for $\mu = \phi\,\text{and}\nu \neq \mu\,,$

$$
\begin{aligned}
\Gamma^{\theta}_{\phi\nu} &= \frac{1}{2}\, r^{-2}\, \{\partial_\phi g_{\nu\theta} + \partial_\nu g_{\theta\phi} - \partial_\theta g_{\phi\nu}\} \\
&= 0\,.
\end{aligned} \tag{A.19}
$$

Finally, $\alpha = \rho = \phi$:

$$
\begin{aligned}
\Gamma^{\phi}_{\mu\nu} &= \frac{1}{2}\, g^{\phi\phi}\, \{\partial_\mu g_{\nu\phi} + \partial_\nu g_{\phi\mu} - \partial_\phi g_{\mu\nu}\} \\
&= \frac{1}{2}\, g^{\phi\phi}\, \{\partial_\mu g_{\nu\phi} + \partial_\nu g_{\phi\mu}\} \\
&= 0\,.
\end{aligned} \tag{A.20}
$$

Thus, all the non-zero Christoffel symbols are:

$$
\boxed{
\begin{array}{llll}
\Gamma^{t}_{rt} = \Gamma^{t}_{tr} = \dfrac{f'}{2f} & & & \\
\Gamma^{r}_{tt} = \dfrac{f\,f'}{2} & \Gamma^{r}_{rr} = -\dfrac{f'}{2f} & \Gamma^{r}_{\theta\theta} = -r\,f & \Gamma^{r}_{\phi\phi} = -r\,f\sin^2\theta \\
\Gamma^{\theta}_{r\theta} = \Gamma^{\theta}_{\theta r} = \dfrac{1}{r} & \Gamma^{\theta}_{\phi\phi} = -\sin\theta\cos\theta. & &
\end{array}
} \tag{A.21}
$$

Appendix B

Scalar field equation of motion

The scalar field equation of motion in a general spacetime is given as,

$$\left[\frac{1}{r^2\sin(\theta)}\partial_\mu\left[\left(r^2\sin(\theta)\right)\ g^{\mu\nu}\partial_\nu\right]\right]\Phi = 0 \tag{B.1}$$

we will run the indices $\mu = \nu$ from 1 till 4 so we can get an equation that explicitly depends on the coordinates $\{t\,,r\,,\theta\,,\phi\}$.

- $\underline{\mu = \nu = t}$

$$\left[\frac{1}{r^2\sin(\theta)}\partial_\mu\left[\left(r^2\sin(\theta)\right)\ g^{\mu\nu}\partial_\nu\right]\right] = \frac{1}{r^2\sin^2\theta}\,\partial_t\left[(r^2\sin\theta)g^{tt}\partial_t\right] = -f(r)\partial_t^2\,. \tag{B.2}$$

- $\underline{\mu = \nu = r}$

$$\begin{aligned}\left[\frac{1}{r^2\sin(\theta)}\partial_\mu\left[\left(r^2\sin(\theta)\right)\ g^{\mu\nu}\partial_\nu\right]\right] =& \frac{1}{r^2\sin\theta}\left[2r\sin\theta\, f(r)\,\partial_r\right]\\ &+\left[r^2\sin\theta\,(\partial_r f(r))\,\partial_r + r^2\sin\theta\, f(r)\,\partial_r^2\right]\end{aligned} \tag{B.3}$$

we will multiply $\frac{1}{r^2\sin\theta}$ into the terms inside the brackets then take out $f(r)$ as a common factor to get,

$$\left[\frac{1}{r^2\sin(\theta)}\partial_\mu\left[\left(r^2\sin(\theta)\right)\ g^{\mu\nu}\partial_\nu\right]\right] = f(r)\left[2r^{-1}\partial_r + (\partial_r\ln f(r))\,\partial_r + \partial_r^2\right]\,. \tag{B.4}$$

- $\underline{\mu = \nu = \theta}$

$$\left[\frac{1}{r^2\sin(\theta)}\partial_\mu\left[\left(r^2\sin(\theta)\right)\,g^{\mu\nu}\partial_\nu\right]\right] = \frac{1}{r^2\sin\theta}\,\partial_\theta\left[\left(r^2\sin\theta\right)\partial_\theta\right] \\ = \frac{r^4\cos\theta}{r^2\sin\theta}\,\partial_\theta + \frac{r^4\sin\theta}{r^2\sin\theta}\,\partial_\theta^2 \\ = r^2\cot\theta\,\partial_\theta + r^2\partial_\theta^2\,. \tag{B.5}$$

- $\underline{\mu = \nu = \phi}$

$$\left[\frac{1}{r^2\sin(\theta)}\partial_\mu\left[\left(r^2\sin(\theta)\right)\,g^{\mu\nu}\partial_\nu\right]\right] = \frac{1}{r^2\sin\theta}\,\partial_\phi\left[(r^2\sin\theta)r^2\sin^2\theta\,\partial_\phi\right] \\ = r^2\sin^2\theta\,\partial_\phi\,. \tag{B.6}$$

To get the full equation we will combine all the results above to one equation,

$$-\,f(r)\partial_t^2\Phi \,+\, f(r)\left[2r^{-1}\partial_r + \left(\partial_r\ln f(r)\right)\partial_r + \partial_r^2\right]\Phi \\ +\, r^2\cot\theta\,\partial_\theta + r^2\partial_\theta^2\Phi \,+\, r^2\sin^2\theta\,\partial_\phi\Phi \,=0. \tag{B.7}$$

Appendix C

Tortoise Coordinates

We had chosen a change in variables (coordinates) that would allow us to simplify the radial equation with relative ease. This change in coordinates also solves the issue of coordinate singularity of the Schwarzschild metric. We saw that the line element in the Schwarzschild metric is given by

$$ds^2 = -\left(1 - \frac{2M}{r}\right)dt^2 + \left(1 - \frac{2M}{r}\right)^{-1} dr^2 + r^2 sin^2(\theta)d\theta^2 + r^2 d\phi^2\,, \tag{C.1}$$

which exhibits a coordinate singularity ar $r = 2M$. If we let $f(r) = \left(1 - \frac{2M}{r}\right)$ then the tortoise coordinates transformation becomes,

$$\hat{R}(r) = \frac{R}{r} \tag{C.2}$$

and

$$dx = \frac{r}{r - 2M}dr\,. \tag{C.3}$$

Solving Eq (C.3) by integrating both sides we get that,

$$x = ln|r - 2M| + C \tag{C.4}$$

where C is a constant that comes from integrating. We can then write r as a function of x as follows,

$$r(x) = e^C e^x + 2M = Qe^x + 2M \tag{C.5}$$

with $Q = e^C$. Taking Eq (C.3) and inserting it into Eq (C.1) we get the result,

$$ds^2 = -\left(1 - \frac{2M}{r(x)}\right)dt^2 + \left(1 - \frac{2M}{r(x)}\right)^{-1} dr^2 + r^2(x)d\Omega^2$$

$$ds^2 = -\left(1 - \frac{2M}{r(x)}\right)dt^2 + \left(1 - \frac{2M}{r(x)}\right)^{-1}\left(1 - \frac{2M}{r(x)}\right)^2 + r^2(x)d\Omega^2\,.$$

Thus, the final form of the line element in these tortoise coordinates is,

$$ds^2 = \left(1 - \frac{2M}{r(x)}\right)\left(-dt^2 + dx^2\right) + r^2(x)d\Omega^2\,. \tag{C.6}$$

Note that there is no longer a singularity since $r(x) \neq 0$ because $Qe^x \neq -2M$ (Q is positive) so that Eq (C.5) is zero.